KfK 3973
September 1985

A Review of Zircaloy Fuel Cladding Behavior in a Loss-of-Coolant Accident

F. J. Erbacher, S. Leistikow
Institut für Reaktorbauelemente
Institut für Material- und Festkörperforschung
Projekt Nukleare Sicherheit

Kernforschungszentrum Karlsruhe

KERNFORSCHUNGSZENTRUM KARLSRUHE
Institut für Reaktorbauelemente
Institut für Material- und Festkörperforschung
Projekt Nukleare Sicherheit

KfK 3973

A Review of Zircaloy Fuel Cladding Behavior in a Loss-of-Coolant Accident

F.J. Erbacher , S. Leistikow

Kernforschungszentrum Karlsruhe GmbH, Karlsruhe

Kernforschungszentrum Karlsruhe GmbH
ISSN 0303-4003

Abstract

The paper reviews the state-of-the-art experimental work performed in several countries with respect to the acceptance criteria established for emergency core cooling (ECC) in a loss-of-coolant accident (LOCA) of light water reactors (LWRs). It covers in detail oxidation, embrittlement, plastic deformation and coolability of deformed rod bundles.
The main test results are discussed on the basis of research work performed at the Karlsruhe Nuclear Research Center (KfK) within the framework of the Nuclear Safety Project (PNS) and reference is made to test data obtained in other countries.
The conclusion reached in the paper is that the major mechanisms and consequences of oxidation, deformation and emergency core cooling are sufficiently investigated in order to provide a reliable data base for safety assessments and licensing of LWRs. All test data prove that the ECC-criteria are conservative and that the coolability of an LWR and the public safety can be maintained in a LOCA.

Ein Überblick über das Zircaloy-Hüllrohrverhalten beim Kühlmittelverluststörfall

Zusammenfassung

Der Bericht gibt einen Überblick über die in verschiedenen Ländern durchgeführten experimentellen Arbeiten im Hinblick auf die für die Notkühlung beim Kühlmittelverluststörfall von Leichtwasserreaktoren aufgestellten Leitlinien. Es werden im einzelnen Oxidation, Versprödung, plastische Verformung und Kühlbarkeit verformter Stabbündel behandelt.
Die wesentlichen Ergebnisse werden auf der Basis der im Kernforschungszentrum Karlsruhe im Rahmen des Projektes Nukleare Sicherheit durchgeführten Forschungsarbeiten diskutiert. Die in anderen Ländern erzielten Ergebnisse werden zitiert. Der Bericht kommt zum Schluß, daß die wesentlichen Mechanismen und Konsequenzen von Oxidation, Deformation und Kernnotkühlung ausreichend erforscht sind und damit eine zuverlässige Datenbasis für Sicherheitsanalysen und Genehmigungsverfahren von Leichtwasserreaktoren geschaffen ist. Alle Versuchsergebnisse zeigen, daß die für die Kernnotkühlung aufgestellten Leitlinien konservativ sind, und daß die Kühlbarkeit eines Leichtwasserreaktors sowie die Sicherheit der Bevölkerung bei einem Kühlmittelverluststörfall gewährleistet sind.

Contents

	Page
Abstract	
Zusammenfassung	
1. Introduction	1
2. Oxidation	3
3. Embrittlement	9
4. Plastic deformation	12
4.1 Single-rod behavior	12
4.2 Multi-rod behavior	14
4.3 Comparison of out-of-pile with in-pile behavior	18
5. Coolability of deformed rod bundles	19
6. Summary	20
7. Conclusion	21
8. Acknowledgements	21
9. References	22
Figures	

1. Introduction

Under the licensing procedures for pressurized water reactors (PWR) evidence must be produced that the impacts of all pipe ruptures hypothetically occurring in the primary loop and implying a loss of coolant can be controlled. The double-ended break of the main coolant line between the main coolant pump and the reactor pressure vessel is the design basis for the emergency core cooling and fuel behavior in a loss-of-coolant accident (LOCA).

Upon rupture of the reactor coolant line a reactor scram is actuated by the reactor protection system. Besides, the reactor is shut down automatically on account of the voids generated in the coolant as a result of pressure relief and the associated loss of moderation capacity. However, as the production of decay heat from fission products continues, reliable long-term cooling of the reactor core is required. After depressurization and evacuation of the reactor pressure vessel emergency core cooling systems (ECCS) supply the reactor core with the emergency cooling water kept in the accumulators and flooding tanks. However, cooling of the fuel elements is temporarily deteriorated until the cooling effect of the emergency cooling water becomes effective. In this time interval Zircaloy fuel rod claddings are heated up by decay heat and some of them may attain temperatures which cause fuel damage.

The temperature transients experienced by the Zircaloy fuel rod claddings depend on a number of boundary conditions e.g. magnitude of the rod power and decay heat, heat transfer from the fuel pellet across the gap to the cladding, external heat transfer from the cladding to the emergency core coolant, etc. Figure 1 illustrates schematically the pressure difference across the cladding and a range of temperature transients for different fuel rods predicted by a conservative evaluation model.

In a large break LOCA the main concerns with respect to Zircaloy fuel rod damage are:

- Oxidation of the Zircaloy which results in embrittlement and possibly fracture of the claddings and may lead to a loss of coolable geometry, release of fuel and fission products, and generation of hydrogen.

- Deformation of the Zircaloy claddings which results in a reduction of the flow subchannel cross sections and may impair coolability.

Licensing authorities have specified core cooling acceptance criteria. The criteria established in the Federal Republic of Germany (FRG) are the following:

1. The calculated maximum peak clad temperature shall not exceed 1200 °C.
2. The maximum clad oxidation shall at no point exceed 17 %.
3. Not more than 1 % of total Zirconium in the clad shall participate in the Zirconium-water reaction.
4. As a consequence of ruptured fuel rods the fission products released shall not be more than:
   - 10 % of noble gases,
   - 3 % of halogens,
   - 2 % of the volatile solid fission products,
   - 0.1 % of other fission products.
5. No changes are permitted in the core geometry which would prohibit sufficient core cooling.

This paper reviews the state-of-the art of ECCS criteria related experimental work performed in several countries. In contrast to other review papers published previously (1,2) and as a supplement to them, this paper covers in more detail the interaction between thermal-hydraulics and cladding deformation and the problems of emergency core cooling of fuel bundles deformed in a LOCA.

Reviewing all test data in detail would be a task beyond the scope of this paper. Therefore, emphasis in this paper is placed on research work performed at the Karlsruhe Nuclear Research Center (KfK) within the framework of the Nuclear Safety Project (PNS).

This review is mainly specific to PWRs, but most of the data base is also applicable to boiling water reactors (BWRs). However, the applicability needs to be assessed in detail under the accident sequences and boundary conditions of a BWR which are different from a PWR and may result in lower peak cladding temperatures and, consequently, lower cladding oxidation and deformation.

2. Oxidation

Steam oxidation is primarily a reaction of the outer surface of the fuel rod cladding. Under accident conditions simultaneous oxidation of the inner cladding tube surface can take place as a result of cladding rupture and steam inward diffusion. Therefore, double-sided exposure was the pessimistic approach in testing the oxidation behavior of Zircaloy tubing in steam. Zircaloy-4 steam oxidation, according to the reaction

$$Zr + 2H_2O \rightarrow ZrO_2 + 2\ H_2; \quad \Delta H = -586\ kJ/Mol,$$

was tested in the temperature range of 600-1600 °C under isothermal and LOCA-typical temperature-transient conditions, predominantly by exposure of PWR cladding tube specimens to a steam flow at atmospheric pressure.

The main test objectives had been

- to measure the kinetics of mass increase, mainly due to oxygen uptake, in the metallic and preoxidized initial surface state,
- to correlate these measurements to the metallographic observation of ZrO_2/ α-Zr (O) double layer growth and to the oxygen content in the β-Zr phase, (Fig. 2),
- to calculate hydrogen and heat production,
- to measure changes in specimen dimensions due to oxidation (and creep deformation),
- to measure changes in mechanical properties due to oxidation, especially gain in strength and loss of ductility (see next chapter on embrittlement).

The following parameters were considered as the main test parameters. Under isothermal conditions: temperature, time, steam flow rate and pressure, hydrogen content of steam, kind of heating, preoxidation, deformation by creep. Under temperature-transient conditions variations of blowdown peak temperatures, heating and cooling rates, holding time at constant temperature were considered in addition within the LOCA transients.

The oxidation kinetics was evaluated by gravimetry. Usually, the mass increase, mainly in oxygen, is given in mg/dm^2 (Fig. 3). 100 mg/dm^2 O_2 correspond to 4,34 μm Zr reacted or to calculated 6,70 μm ZrO_2 formed. Since at high temperatures oxygen is diffusing into the metallic matrix the scale

thickness of ZrO_2 is observed to be about 25 % lower. The hydrogen evolution method, but also scale growth measurements were occasionally applied. The following results will show that due to the formation of an adherent, sub-stoichiometric, black ZrO_2 scale as the main oxidation product, the reaction rate slows down with growing scale thickness - a behavior which is typical of protective oxide scale growth at high temperatures following a cubic or parabolic time dependency.

The literature on Zircaloy oxidation was reviewed by Scatena (3), Parsons and Miller (4), and Ocken (5). Experimental work was performed by many investigators all over the world.

Cathcart et al. (6) measured besides the kinetics of the ZrO_2 scale, the α-Zr(O) layer, and combined layer growth as well as the diffusion coefficients of oxygen in the α- and β-Zr-phases. Parabolic rate coefficients were given for the temperature range above 1000 °C. While Biederman et al. (7) used resistance heating of the specimens under oxidation, Urbanic and Heidrick (8) used inductive heating in their experimental studies. Both groups found lower activation energies in the Arrhenius presentation of their results. Similar investigations were performed in Japan by Suzuki and Kawasaki (9) and in the United Kingdom by Brown et al. (10) who used Zircaloy-2 as the test material.

Our investigations were performed in tubular furnaces in the range of 600 - 1300 °C, $\leq$ 15 min (11). Parabolic functions were measured for the oxygen uptake (see Fig. 3) and ZrO_2, α-Zr(O), and for combined layer growth; they are valid above 1000 °C, but applicable as approximation at lower temperatures as well. Rate equations were established and allow to calculate the corresponding heat and hydrogen production and to verify codes based on first principles. Regarding their parabolic character and trend to considerably lower oxidation rates, compared to the Baker-Just equation (12) (Fig. 4), these test results are consistent with the results mentioned above. A trend towards cubic kinetics was observed below 1000 °C due to a transformation of the oxide structure. The gradual change over to cubic kinetics is finally completed at and below about 800 °C. Breakaway has not yet shown up within the LOCA relevant time-temperature range.

Ocken (5) defined two groups of data according to the corresponding method of specimen heating. A correlation based on experiments with internal specimen

heating was proposed to replace the conservative Baker-Just equation. However, a strong argument in support of the investigations involving external heating (6,9,10,11) is the better defined temperature control in a furnace compared to resistance (7) and inductive heating (8). The strong temperature dependence of the oxidation in combination with difficulties in precise specimen temperature measurement may well account for the observed scatter band in published data.

Computer codes were developed to model the oxidation of Zircaloy. The SIMTRAN I (13,14) and ZORO 1 (15) codes are finite difference treatments of the three-phase diffusion problem which assume equilibrium interface oxygen concentrations and calculate the total oxygen uptake as well as interface movements and oxygen concentration profiles across the tube wall. SIMTRAN was developed further into MULTRAN, a multiphase version (16), and PRECIP II (17). A more recently developed, similar finite difference code, PECLOX (18) is capable of treating fuel/cladding interaction in combination with external steam oxidation of the cladding on the basis of oxygen diffusion with moving interfaces.

Preexisting oxide scales formed by corrosion under reactor operation conditions have an influence on Zircaloy oxidation under LOCA conditions, depending essentially on their thicknesses and physical states of protectiveness. While oxide scale thicknesses can be simulated by high temperature steam oxidation during relatively short time of preexposure, their physical state is in reality depending on various in-pile parameters (temperature, pressure, heat transfer, environment, radiolysis etc.) and therefore can not be reproduced in a simple manner under out-of-pile conditions. Nevertheless oxide scales, artificially prepared by steam exposure at 350 - 600 and 800 °C in our laboratory (11), showed a protective effect on LOCA oxidation which vanished by excessive scale growth and at temperatures above 1100 °C.

The need to approach a realistic exposure at time-at-temperature during which scale cracking due to oxide growth stresses, changes in temperature and phase transformations in the metal and oxide can exert a special influence on oxidation kinetics was the reason for oxidation testing in steam under LOCA-similar transient conditions.

Experimental results of some temperature transients were reported (6,7,19).

LOCA transients and simple temperature ramps could be roughly evaluated on the basis of isothermal results, except for "anomalous" effects caused by oxide phase transformation and duplex $\alpha+\beta$ interphase layer formation. In own investigations with inductively heated specimens a first peak, a second ramp and an additional holding at temperatures between 700 and 1200 °C were tested (20). In a first approximation the oxidation is determined by time-at-temperature and it compares fairly well with predictions based on the isothermal behavior. The results exhibit a remarkable difference between our isothermal results and those obtained in the course of the 3 min-transients. Expressed in percentages, a reduction of a quarter (100 -1200 °C) to one third (900 - 1000 °C) in oxygen uptake was measured compared with isothermal conditions (Fig. 5). As in the isothermal exposure, the protective effect of pre-existing scales degrades above 1100 °C, but under transient conditions a broad scatter in local behavior precludes a reliable deterministic evaluation.

The effect of creep deformation on oxidation kinetics also was considered. Whereas Furuta et al. (21) report enhanced general oxidation after straining by Zircaloy-4 tube burst or tensile tests, Bradhurst and Heuer (22) have found no direct influence on Zircaloy-2 oxidation outside of oxide cracks.

The latter was confirmed by own investigations of the oxidation behavior of internally pressurized tube capsules (600-1300 °C, 150 bar) (23). By interruption of such creep tests at 800 °C (Fig. 6) and 900 °C, a comprehensive description of oxide crack formation (Fig. 7) in respect to density and width could be given as a function of time and internal pressure: At high pressure numerous, narrow cracks were formed; at low pressure the cracks were less in number, but wider. Access of steam to fresh metallic surfaces within the cracks resulted in a linear correlation between strain and additional oxidation. As the deformation was found to proceed by widening of early-formed cracks, this indicated that deformation concentrates on the cracked, mechanically weak regions which induces premature necking of the material far below the limit of uniform elongation of the base material (Fig. 8).

According to a literature review growth stresses induced by oxide scale formation on Zircaloy may cause or contribute to deformation under applied stress, especially if nitrogen is present in oxidizing atmospheres (24). This could have played a role in the reported ductilizing effect of oxidation on Zircaloy-4 (25), which was deduced from tensile, creep, and some tube burst

tests performed in air, in comparison to vacuum. Own results (26) have confirmed that air is an inadequate medium to study oxidation at temperatures > 900 °C in relation to the mechanical behavior, since air grown scales show no load bearing capability.

Steam grown oxide layers exert a clear strengthening effect (Fig. 9); this was realized by a comprehensive investigation of the creep-rupture behavior of tube capsules under constant internal argon pressure and externally exposed to argon or steam (600-1300 °C, 2-150 bar) (27). The increase in strength (due to the oxide and α-Zr(O) formation as well as oxygen dissolution in the remaining β-phase) overcompensates the decrease by oxidative consumption of the load bearing wall thickness, i.e. the matrix material. The oxidized specimens showed a considerable reduction in circumferential burst strain compared to similar tests in argon. This reduction in ductility is observed already after small amounts of oxygen diffused into the base metal and reacted by forming a strong ZrO_2 jacket (metal-oxide compound of "sandwich" structure) on the tube circumference.

The results of this investigation have contributed to the development of the NORA model (28). In this code the influence of oxidation on the deformation of Zircaloy is treated with a homologous temperature applied in order to simulate the modified microstructure of oxidized material. In the failure criterion an empirical function for strain reduction of oxidized material is used. A comprehensive investigation of the mechanical behavior of oxygen-containing Zircaloy, performed with oxidized and subsequently oxygen equilibrated specimens, was performed by Kassner et al. (29).

The chemical interaction between the cladding and the fuel was investigated by Hofmann et al. (30,31), who quantified the kinetics and described the sequence of reaction layers. However, without solid contact or in the presence of oxide scales on the inner cladding surface the reaction is prevented. So, under LOCA aspects, the chemical interaction between the fuel and the cladding is unimportant, since cladding lift-off under internal pressure reduces the area of fuel/cladding contact. From the simulated volatile fission products only iodine above critical concentrations can cause low ductility failure of the cladding due to stress corrosion cracking (Fig. 10). Under LOCA conditions, however, an influence on burst strain is not very probable (32).

Investigations performed by Furuta et al. (33,34) related to the internal oxidation of the cladding by steam penetrating through the burst opening of ruptured fuel rods. In the vicinity of the rupture these authors recorded thicker internal scales compared to the external ones, and thicker than calculated under the post-rupture conditions. The thickness, local distribution and cristallographic structure of the internal oxide were evaluated as a function of time, steam temperature and flow rate, and length of rupture opening.

In order to simulate the conditions of internal oxidation, such as stagnation, consumption, and hydrogen enrichment, isothermal tests were performed in steam-hydrogen mixtures using short tube specimens (35). "Normal" oxidation resulting in dense, monoclinic oxide, relatively thick α-Zr(O) layer, basket weave prior β-phase microstructure, relatively high mid-wall oxygen concentration, and low hydrogen uptake, above critical hydrogen fractions in the atmosphere changed to another mode, found to be typical of internal cladding oxidation: Its features were porous oxide composed of monoclinic plus tetragonal phases, a relatively thin α-Zr(O) layer, martensitic prior β-phase microstructure, relatively low mid-wall oxygen concentration, and high hydrogen uptake, which dominated the reduction in specimen ductility, as observed in ring compression tests.

Integral tests conducted under in-pile conditions generally confirmed the results of out-of-pile separate effects investigations. In the FR2 in-pile tests, performed by Karb et al. (36), during which temperatures up to 1050 °C were reached, the resultant external cladding oxidation in general (Fig. 11) was not influenced by the pre-irradiation conditions. Premature breakaway was observed locally (37). Internal steam oxidation was found to be restricted to about $\pm$ 10 cm around the burst elevation. But here the oxide scales were often much thicker than expected from the time and temperature of exposure to the penetrating steam, and for pre-irradiated rods thicker than the external scale.

On the whole, internal oxidation is considered as relatively unimportant under LOCA conditions. Oxidation by fuel can be treated conservatively to result in an equal penetration of the Zircaloy matrix by oxygen-rich α-Zr(O), compared to the external oxidation. But since no oxide scale is formed, the total reaction turnover and the resulting reaction heat is far below

the contribution by external oxidation. Oxidation by penetrating steam can cause even thicker oxide scales than externally, but is locally restricted to the vicinity of the burst opening, and is therefore only a small contribution to the total oxidation of the cladding tube.

A rough estimate of the safety margin for a LOCA can be based on the comparison of the 17 % criterion and own results of isothermal oxidation experiments. These tests approximate the complicated real oxidation sequence of

- external preoxidation under normal reactor operation conditions, i.e. growth of ZrO_2 scales of 100 μm or less
- LOCA transient external oxidation, eventually moderated by the protective effect of the preexistent scale
- internal LOCA transient oxidation

by double-sided exposure of metallic tubing.

The resultant durations of isothermal exposure until 17 % wall consumption is achieved (which corresponds to 1403 mg/dm^2 total O_2 uptake on both sides of the 725 μm tube wall) are as follows: 70 minutes at 1000 °C, 27 minutes at 1100 °C, 9 minutes at 1200 °C and 4 minutes at 1300 °C. That appears to be a relatively long time span. However, since the 17 % oxidation limit is linked by the Baker-Just equation to embrittlement considerations, the criterion itself and the permissible accident durations will be considered again in the next chapter on embrittlement.

LOCA analyses by pessimistic evaluation models show that the peak cladding temperature is lower than 1000 °C and the time duration at temperature shorter than 2 minutes (see Fig. 1). Therefore, it can be concluded that the 17 % criterion is very conservative and oxidation is of no concern in a LOCA.

3. Embrittlement

The total amount of oxygen and its distribution within the tube wall determine the degree of cladding embrittlement. In case of mechanically defect oxide scales also hydrogen uptake contributes to the reduction in ductility. The influence of hydrogen was studied by Uetsuka et al. (38, 39), who analyzed the hydrogen content of ring sections from LOCA tested fuel rod simulators in relation to their ductility in the compression test. The spread of an embrittled zone was comparable to the zone of internal oxide. However, peaks

in hydrogen content (analyzed 15-45 mm above and below the rupture opening) coincided with the maximum loss in ductility so that embrittlement was considered to be mainly due to the hydrogen uptake, for which a maximum of 2050 wt. ppm was found. The oxidation temperature and steam flow rate determined the distance of these peaks from the rupture opening. For temperatures above 1000 °C, the minimum hydrogen content causing brittle fracture was 200-300 wt. ppm; for duplex $\alpha+\beta$ phase microstructures formed below 1000 °C the embrittling content was 500-750 wt. ppm. Tests with UO_2 pellets filled simulator rods identified no additional effect of the H_2O-UO_2 reaction and hardly observable differences between the behavior of cooled and quenched rods.

Hobson and Rittenhouse (40) evaluated isothermal steam oxidation tests in terms of the time-temperature dependence of ZrO_2 plus α-Zr(O) combined layer penetration and proposed an integration method for dealing with transients. Ring sections cut from the specimens were hardness and impact compression tested in order to identify cladding embrittlement under steam bursts, hydrodynamic forces and tube rupture. Various other correlations for the description of the extent of oxidation have been used to define limiting values of parameters which quantify the maximum permissible embrittlement. Scatena (3) compares the different approaches under this aspect.

The present ECCS-criteria are limiting oxidation and hence embrittlement by defining the maximum LOCA temperature as 2200 °F or 1200 °C and the permissible equivalent cladding reacted (ECR) as 17 %. Embrittlement related investigations performed by Furuta, Uetsuka and Kawasaki, summarized in (41), comprised tube oxidation/ring compression tests, rod burst/ring compression tests and rod burst/bottom flooding tests. It was stated that a 15 % ECR criterion calculated by the Baker-Just correlation was adequate to account for the embrittling effects of oxygen uptake, hydrogen absorption in the interior of the burst cladding, and constraint stresses during the thermal shock of quenching.

A lot of work has been done to check the validity under various simulated accident and post-accident conditions. It was found that the embrittlement is also dependent on the amount and distribution of oxygen in the β-phase. Consequently, Pawel (42) calculated oxygen concentration profiles as a function of the extent of oxidation and temperature. In comparison to embrittlement data he proposed 0.7 wt.% of average oxygen concentration in β as

embrittlement limit for oxidation temperatures above 1260 °C, and 95 % fractional oxygen saturation in β as the limit for oxygen uptake at lower temperatures.

Chung and Kassner (43) exposed fuel rod simulators to isothermal steam oxidation and to rupture under internal pressure. The cladding response to bottom flooding with water was compared with the measured widths of the ZrO_2 and α-Zr(O) layer and the calculated oxygen profile across the wall. Good correlation of the fracture behavior was found for the following proposed failure criterion: A cladding with a minimum of 0.1 mm of β-phase with 0.9 wt.% or less of oxygen is capable of withstanding thermal shocks during LOCA reflood. Slow cooling resulted in slightly higher ductility, allowing 1.0 wt.% in this fractional β-phase layer. Chung and Kassner also investigated the capability of the cladding to withstand loads arising from handling, storage and transport of fuel rods in impact, tension, and diametral compression tests performed at ambient temperature. Since the magnitude of realistic loads is unknown, the arbitrary energy value of 0.3 J of impact at 300 K was chosen for evaluation of an interim failure criterion: Failure is expected to occur if less than 0.3 mm of the β-phase with an oxygen content of 0.7 wt.% or less remains. Haggag (44) evaluated in-pile experiments and out-of-pile embrittlement studies of isothermally oxidized fuel rod simulators. The data were compared to different embrittlement criteria. The observed thermal shock failures were predicted by all of them, whereas some handling failures were predicted by any of the criteria checked. It was stressed that the Chung-Kassner criteria require a more sophisticated calculation of the distribution of oxygen concentration than the simpler older criteria, but offer the advantage that they distinguish between quenching and handling failures.

Whereas the 17 (15) % ECR criterion might be inadequate for excessive wall thinning and in case of a contribution by internal oxidation, the Chung-Kassner criteria are applicable to the ballooned and burst region of a fuel rod. Our SIMTRAN oxygen profile calculations, based on own oxidation experiments, showed that by double-sided steam oxidation of non-preoxidized tubing the limiting oxygen concentrations mentioned above in the β-phase are reached under isothermal conditions at 1200 °C within 5 minutes (Fig. 12), which is equivalent to oxidation under transient conditions with a holding times at 1200 °C during about 8 minutes.

Due to the high cooling efficiency of the ECCS these time durations at temperature are far from being reached in a LOCA. Therefore, no concern exists about the integrity of the fuel in a LOCA.

4. Plastic deformation

4.1 Single-rod behavior

A large number of single-rod tests were performed in many countries (45-62). The main objectives of these tests were to investigate the effects of internal pressure, heating rate, temperature, temperature-nonuniformities and oxidation on the cladding deformation over a wide range of parameters. The test results have been used to develop and verify various cladding deformation models. All test data are consistent. The essential conclusions will be discussed in the following paragraphs on the basis of test results obtained under the REBEKA program. In this program cold worked, stress relieved Zircaloy-4 cladding tubes of 10.75 mm outer diameter and 0.725 mm wall thickness were used.

Figure 13 shows the burst temperature of Zircaloy cladding tubes plotted versus the burst pressure. The curves in this diagram and in Figs. 14, 15 and 19 are the result of a deformation model developed within the REBEKA program which was verified by numerous single rod tests (63, 64). For identical heating rates a higher rod internal pressure leads to a lower burst temperature. The diagram shows the influence of the heating rate on the burst temperature over the whole pressure and temperature ranges investigated. High heating rates give higher burst temperatures than low heating rates.

Figure 14 shows the circumferential burst strain plotted versus the burst temperature. The general tendency indicates a first maximum of strain to occur at approximately 820 °C in the range of transition from the hexagonal α--phase of Zircaloy into the ($\alpha+\beta$) mixed phase, a minimum of strain in the intermediate ($\alpha+\beta$) range at approximately 920 °C, and a second maximum, depending on the heating rate, in the upper ($\alpha+\beta$) range and in the body-centered cubic β-phase, respectively, of Zircaloy. The diagram makes evident the influence of the heating rate on burst strain. In the α-range the burst strain increases with the heating rate becoming smaller, in the β-range the burst strain decreases with the heating rate getting lower. This reversal of

the strain behavior in the β-range as a function of the heating rate is attributable to the influence of oxidation of Zircaloy.

It has been found that Zircaloy cladding deformation is extremely sensitive to temperature. Figure 15 shows that even a small change by $\pm$10 K in the cladding temperature changes the time-to-burst by some $\pm$40 %. Since the time of maximum cladding temperature in a LOCA transient is limited by the cooling efficiency, minor cladding temperature variations may result in a cladding burst and only in a very small cladding deformation, respectively. This makes evident the great difficulties encountered in predicting with sufficient accuracy cladding strain and failure by deterministic thermal-hydraulic analyses. The required accuracy of the cladding temperature of at least $\pm$10 K in respect to cladding deformation cannot be achieved with the existing thermal-hydraulic computer codes.

In single-rod tests with the shroud heated in order to produce uniform temperatures on the cladding circumference Zircaloy has been found to show a specific deformation behavior in the α-phase range due to its texture and anisotropy. Circumferential elongation under internal overpressure is accompanied by an axial material flow, which leads to a shortening of the Zircaloy tube. Figure 16 shows that the cladding length changes as a function of the burst temperature. The diagram reveals remarkable cladding tube shortening in the α-phase range.

In single-rod tests in which the shroud remained unheated the heat transfer from a fuel rod to the coolant and the temperature differences developing on the cladding tube circumference due to unavoidable non-uniform gap widths between the pellets and the cladding were simulated. Under the said conditions which are representative of a LOCA, straining occurs first on the hot side. As a consequence, the hot side will shorten, forcing the cladding into close contact with the heat source and lifting the opposite colder side of the cladding away from it. In this way, circumferential differential temperatures on the cladding are intensified during deformation, and wall thinning is concentrated at the hot spot, resulting in a relatively low total circumferential strain.

Figure 17 illustrates the described deformation behavior of the Zircaloy claddings. Figure 18 is a photograph of a Zircaloy tube deformed under azi-

muthal temperature difference and cooling.

It has been demonstrated that in case of deformation of Zircaloy claddings in the α- and $(\alpha+\beta)$ phases a systematic relationship exists between the circumferential burst strain and the azimuthal temperature difference on the cladding tube: Small azimuthal temperature differences on the cladding tube cause a relatively homogeneous decrease of the cladding tube wall thickness along the circumference and, consequently, lead to relatively large burst strains; large azimuthal temperature differences occurring in the course of deformation lead to a preferred reduction in wall thickness on the hot part only of the cladding tube circumference and hence to relatively low burst strains. Figure 19 shows in quantitative terms the influence of azimuthal temperature differences on the circumferential burst strain. The figure makes clear the great influence of azimuthal temperature differences on reducing the burst strain. Therefore, the size of azimuthal temperature differences along the cladding tubes circumference is one of the most decisive parameters influencing cladding tube strain, flow blockage and coolability in a LOCA.

4.2 Multi-rod behavior

Several multi-rod test programs were performed, mainly in the Federal Republic of Germany, in France, Japan, the United Kingdom and the USA. The main objectives of these tests were to investigate the interaction of thermal-hydraulics and cladding deformation, the consequences of rod-rod interactions within the rod bundle, the effects of grid spacers, and finally, the maximum flow blockage. The test data obtained have been used in licensing procedures for PWRs.

Reviewing all multi-rod tests in detail is beyond the scope of this paper. Therefore, the essential conclusions will be discussed on the basis of test results obtained within the REBEKA program. For comparison some other tests are selected which provided an adequate LOCA simulation, i.e. internal heating with pellet/clad gap, heated length exceeding at least one intergrid span, representative thermal-hydraulics.

Table I summarizes some of the multi-rod tests performed up to now. From the individual test series only those are listed which have the potential for maximum ballooning, i.e. burst in the high α-phase of Zircaloy around

800 °C. The differences in the test results are mainly due to different thermal-hydraulic test conditions. All test data are in principle consistent with the understanding elaborated within the REBEKA program. Table II summarizes the REBEKA multi-rod burst tests.

The important generic result of all multi-rod tests is that the deformation behavior of the Zircaloy cladding tubes in a bundle geometry follows the mechanisms investigated in single-rod tests. The burst temperatures and burst pressures determined in the bundle tests as well as the burst strains as a function of the azimuthal cladding temperature difference agree with the burst data measured on single rods (see Figs. 13 and 19).

Effect of heat transfer on clad ballooning

It has been found in the REBEKA tests that the circumferential burst strain becomes the smaller the higher the heat transfer from the cladding tube to the coolant is (see Tab. II). This is the result of tube bending occurring in case of azimuthal temperature differences where the hot side of the cladding tube during deformation continues to be in more or less close contact with the inner heat source and the opposite cold side is deformed in such a way that it continuously moves away from the inner heat source (see Fig. 18). Via this mechanism heat transfer, which is intensified during reflooding, leads to an increase in azimuthal temperature differences on the cladding tube and, consequently, to a reduction of the circumferential burst strain.

Figure 20 illustrates the influence of heat transfer on Zircaloy cladding deformation under the simplified assumption of full eccentricity of the pellet within the cladding from the start of the heat-up phase. The diagram makes clear that bundle tests performed in very low heat transfer by steam cooling must lead to relatively high burst strains (see Tabs. I and II) and that tests with heat transfer coefficients typical of the reflooding phase of a LOCA (> 50 W/m^2K) result in relatively low burst strains.

In all multi-rod tests performed under heat transfer conditions typical of a LOCA azimuthal temperature differences of approx. 30 K have been observed at the time of burst which limits the mean circumferential burst strain of the Zircaloy cladding tubes to values around 50 % (see Figs. 14, 19 and 25).

Effect of coolant flow direction on flow blockage

The flow blockage in a rod bundle caused by the ballooned cladding tubes is influenced by the axial displacement of the burst points between two spacers. If these points are distributed over a great length the resulting flow blockage becomes relatively small, but if the burst points are located closely together a relatively great flow blockage develops for the same mean circumferential burst strain. Since plastic deformation of Zircaloy cladding tubes reacts very sensitively to the cladding tube temperature (see Fig. 15), the axial displacement of the burst points is decisively determined by the axial profile of the cladding tube temperature prevailing between two spacers. The profile of cladding tube temperature is among others the result of the thermodynamic non-equilibrium in two-phase flow and its being influenced by the spacer grids. Moreover, it is determined by the direction of flow, i.e. by the fact whether in the process of cladding tube deformation the flow is unidirectional or whether it changes its direction between the refill and reflooding phases.

The heat transfer between the rods and the steam-water droplet mixture downstream of the quench front takes place almost exclusively by convection. Since the heat transfer from the cladding tube wall to the steam is substantially higher than from steam to water droplets, a thermodynamic non-equilibrium is established during the reflooding phase in two-phase flow, i.e., the steam is superheated along the coolant channel. In the bundle tests steam superheating up to approximately 500 K was measured. Moreover, it has been found that downstream of a spacer grid the water droplets are more finely distributed due to droplet breakup at the grid. On account of the greater droplet surface involved, this results in a more effective heat sink for the superheated steam. The turbulence enhancing effect of the spacer grids gives rise to intensive mixing of the water droplets with the superheated steam and, consequently, to a reduced degree of steam superheating downstream of each spacer grid. However, on the way to the next spacer grid in the direction of flow, the degree of superheating increases again which leads to the development of an axial temperature profile between two spacer grids (82).

The improved heat transfer around the spacer grids decreases substantially the cladding tube strain in the vicinity of the spacer grids, especially downstream of the spacer grids. The axial zone of displacement of the burst

points between the spacer grids is essentially determined by the fact whether the direction of flow remains unchanged during deformation or whether it undergoes variations.

The direction of coolant flow in a reactor core during a LOCA depends mainly on the design and availability of the emergency core cooling systems and their thermal-hydraulic interaction with the primary loops. Therefore, in the individual core zones different cooling and flow conditions may establish during the refill- and reflooding phases. Besides local flow variations and countercurrent flow situations of steam and water two main and limiting coolant flow directions can be characterized in terms of their influence on the cladding deformation: reversed flow from the refill to the reflooding phase and undirectional flow during the refill and reflooding phases.

Figure 21 makes evident for REBEKA 5 the consequence of reversed flow from the refill to the reflooding phases on the deformation pattern. Due to inhomogeneities in the rod bundle resulting from locally different rod powers and cooling conditions the individual rods showed different plots of cladding tube temperatures versus time. This implies different times of burst for the individual rods and - because the cladding tube temperature maxima occurring between the spacer grids are shifted as a function of the time due to reversed flow - likewise an axial displacement of the burst points. The burst points are distributed over an axial length of 242 mm around the axial midplane which results in a relatively low flow blockage of 52 %.

Figure 22 shows the deformation pattern obtained in the REBEKA 6 bundle test in which the direction of coolant flow was maintained for the refill and reflooding phases. Unlike in REBEKA 5, the temperature maximum was shifted towards the upper spacer grid from the beginning of the experiment. After the temperature profile has developed in the refill phase, the temperature maximum remains largely stationary in its axial position. Consequently, the burst points are arranged more closely to each other and thus give rise to a larger flow blockage. It is apparent from the figure that the burst points are displaced solely over an axial length of 140 mm and shifted towards the upper spacer grid. The resulting flow blockage is 60 %, i.e., it is greater than in the case of reversed flow direction.

In the REBEKA 7 test, which was performed also under unidirectional flow,

maximum rod-rod interaction and cladding deformation developed. This test resulted in the highest possible flow blockage of 66 % (Fig. 23).

Based on the out-of-pile and in-pile bundle tests performed up to now it can be concluded that under thermal-hydraulic boundary conditions typical of emergency core cooling systems operating according to design the best estimate maximum flow blockage in a LOCA is not greater than 70 %.

4.3 Comparison of out-of-pile with in-pile behavior

In order to check the quality of simulation of the out-of-pile tests involving electrically heated fuel rod simulators, in-pile tests were performed to investigate the influence of a nuclear environment on the mechanisms of fuel rod deformation and failure.

In the FR-2 reactor of KfK single-rod tests were performed in steam using 500 mm long unirradiated as well as irradiated rods (36). The burst data of these in-pile tests, i.e., the burst pressures, burst temperatures and burst strains, are in good agreement with the REBEKA out-of-pile test data. The relatively low burst strains found in the FR-2 tests are also the result of azimuthal cladding temperature differences. Figure 24 is a plot of the circumferential burst strain versus the azimuthal difference at maximum clad temperature. It is evident from the diagram that significant temperature variations on the cladding circumference occurred. No influence was found of the fragmented fuel of the irradiated fuel rods on the azimuthal cladding temperature difference and the resulting burst strain. The burnup had no influence on the burst data, and a difference between the unirradiated and the previously irradiated test rods was neither observed. In the regions with major clad deformations of the pre-irradiated rods fragmented fuel pellets were found crumbled within the fuel rod. There is experimental evidence that the fuel fragments moved at the time of burst and did not influence the deformation behavior.

The circumferential burst strains of the FR-2 and other in-pile tests are plotted in Fig. 25: EOLO tests in ESSOR (56), tests in PBF (51), NRU (69) and PHEBUS (68). All results are well within the scatter band of the FR-2 in-pile and REBEKA out-of-pile test results and do not indicate an influence of the nuclear boundary conditions on the cladding deformation in a LOCA.

Comparing out-of-pile and in-pile tests it can be concluded that the results of out-of-pile tests performed under LOCA typical boundary conditions are representative of nuclear fuel rods and can be used for the LOCA analysis under licensing procedures for PWRs.

5. Coolability of deformed rod bundles

Flow blockages produced by ballooned and burst claddings change the cooling mechanisms downstream of the blockage. The increased flow resistance in the blocked region results in a reduction of the coolant mass flow and heat transfer. On the other hand, droplet breakup and turbulence enhancement occurring at the blockage improve heat transfer. It depends on a number of boundary conditions which of these effects is predominant (82).

In thermal-hydraulic bundle experiments, i.e. FEBA (80), THETIS (79), FLECHT-SEASET (77), SCTF (78) and CCTF (81), the temperature and quench behavior of deformed rod bundles were investigated (see Table III). Ballooned fuel rod claddings were simulated by sleeves fixed on the outer surface of conventional heater rods.

Within the FEBA program flooding tests with forced feed were performed under transient LOCA conditions on a 5x5 bundle with coplanar conical sleeves. Figure 26 shows cladding temperature transients in the blocked and unblocked regions for a flooding rate of 3.8 cm/s in the cold bundle and a blockage ratio of 62 % in the blocked region. It is evident from the diagram that under the given conditions the effect of water droplet breakup, which improves the heat transfer, overcompensates the degrading effect of mass flow reduction with the consequence that the cladding temperature downstream of the blocked region is somewhat lower compared to that in the unblocked region.

Figure 27 shows corresponding plots for a blockage ratio of 90 % in the blocked region. It makes evident that under these severe conditions the coolant mass flow reduction overshadows the two-phase cooling enhancement effect. However, the temperature rise downstream of the blockage and the delay in quench time are moderate. From these results it can be concluded that rod bundles blocked up to 90 % are still coolable.

The FEBA results are consistent with the results from other tests which were performed with larger bundles, larger bypass regions and partly with gravity feed. The higher temperature rise found in the THETIS blockage experiment is mainly the consequence of a more severe blockage shape and a low rod power both of which tending to furnish very conservative results.

In all these thermal-hydraulic tests on blocked bundles conventional electrical heater rods were used with no gap between the stainless steel cladding and the inner heating element. It has been shown in the REBEKA- and SEFLEX-program that such gapless heater rods exhibit higher peak cladding temperatures and longer quench times compared to nuclear fuel rods. In addition, it has been found that burst cladding tubes quench even earlier compared to intact cladding tubes and generate secondary quench fronts (83).

These recent results prove again that in fuel elements blocked up to 90 % by ballooned and burst Zircaloy claddings the coolability in a LOCA can be maintained.

6. Summary

The essential results of this review on Zircaloy fuel cladding behavior under boundary conditions typical of a large break LOCA can be summarized as follows:

- The Baker-Just equation describes the oxidation kinetics in a very conservative manner.
- The extent of oxidation stays within the 17 % limit of the ECC-criteria even after extended preoxidation and transient exposure at maximum temperature (10 min, 1200 ^{o}C).
- ECC-criteria are sufficiently conservative to limit embrittlement due to oxygen and hydrogen absorption with respect to thermal shocks during quenching.
- The circumferential burst strain of the cladding is kept relatively small due to temperature differences on the cladding circumference.
- The cooling effect of the ECCS increases temperature differences on the cladding tube circumference and limits in this way the mean circumferential burst strains to values around 50 %.
- Uni-directional coolant flow during the refilling and reflooding phases results in the highest possible flow blockage of approximately 70 %.

- In-pile test data are consistent with the out-of-pile data and do not indicate an influence of the nuclear environment on cladding deformation.
- In fuel elements blocked up to 90 % by ballooned and burst Zircaloy claddings the coolability in a LOCA can be maintained.

7. Conclusion

The results elaborated worldwide on oxidation, deformation and coolability in a LOCA constitute a reliable data base and an important input for the safety assessment of LWRs.

Thermal-hydraulic analyses of emergency core cooling by pessimistic evaluation models show that in a PWR the majority of the fuel rods reach peak cladding temperatures lower than 700 °C and that only the relatively few high rated fuel rods which make up less than 1 % in the whole reactor core attain peak cladding temperatures of approx. 1000 °C. The percentage of fuel rods with peak cladding temperatures above 800 °C is less than 10 %. The internal rod pressure of prepressurized PWR fuel rod claddings in a LOCA is calculated to be around 60 bar depending on the fuel rod design and burnup and the time period at maximum cladding temperatures is limited to less than 2 minutes due to the high efficiency of the emergency core cooling systems.

Therefore, it can be concluded that the ECC-criteria established by licensing authorities are conservative and that the coolability of an LWR and the public safety can be maintained in a LOCA.

8. Acknowledgments

The efforts of many have contributed greatly to the work reported here. The authors wish to gratefully acknowledge their outstanding contributions.

The research work at the Karlsruhe Nuclear Research Center (KfK) was sponsored by the Nuclear Safety Project (PNS). The authors gratefully acknowledge the support by A. Fiege.

9. References

(1) Mann, C.A., Hindle, E.D., Parsons, P.D., "The Deformation of PWR Fuel in a LOCA." United Kingdom Atomic Energy Authority Northern Division Report ND-R-701 (S), April 1982.

(2) Pickman, D.O., Fiege, A., "Fuel Behavior under DBA Conditions", KfK 3880/1, December 1984, pp. 73 - 94.

(3) Scatena, G.J., "Fuel Cladding Embrittlement During a Loss-of-Coolant Accident". NEDO-10674, October 1972.

(4) Parsons, P.D., Miller, W.N., "The Oxidation Kinetics of Zirconium Alloys Applicable to Loss-of-Coolant Accidents". A Review of Published Data. ND-R-7(S), October 1977.

(5) Ocken, H., "An Improved Evaluation Model for Zircaloy Oxidation". Nuclear Technology 47 (1980), pp. 343-357.

(6) Cathcart, J.V. et al., "Zirconium Metal-Water Oxidation Kinetics IV. Reaction Rate Studies". ORNL/NUREG-17, August 1977.

(7) Biederman, R.R., Sisson Jr., R.D., Jones, J.K., Dobson, W.G., "A Study of Zircaloy-4-Steam Oxidation Reaction Kinetics". EPRI NP-734, April 1978.

(8) Urbanic, V.F., Heidrick, T.R., "High Temperature Oxidation of Zircaloy-2 and Zircaloy-4 in Steam". J. of Nuclear Materials 75 (1978), pp. 251-261.

(9) Suzuki, M., Kawasaki, S., Furuta, T., "Zircaloy-Steam Reaction and Embrittlement of the Oxidized Zircaloy Tube under Postulated Loss-of-Coolant Accident Conditions". JAERI-M 6879, December 1976.

(10) Brown, A.F., Tucker, M.O., Healey, T., Simpson, C.J., "Oxide/α and α/β Phase Interface Advance Kinetics in Steam Oxidized Zircaloy-2" RD/B/N4882, July 1980.

(11) Leistikow, S., Schanz, G., v. Berg, H., "Kinetics and Morphology of Iso-

thermal Steam Oxidation of Zircaloy-4 at 700-1300 °C". KfK 2587, March 1978.

(12) Baker, L., Just, L.C., "Studies of Metal-Water Reactions at High Temperatures. Experimental and Theoretical Studies of the Zirconium-Water Reaction". ANL-6548, May 1962.

(13) Malang, S., "SIMTRAN-I - A Computer Code for the Simultaneous Calculation of Oxygen Distributions and Temperature Profiles in Zircaloy During Exposure to High-Temperature Oxidizing Environments". ORNL-5083, November 1975.

(14) Malang, S., Schanz, G., "Description and Verification of SIMTRAN I, a Computer Code for the Calculation of High Temperature Steam Oxidation of Zircaloy". Specialists Meeting on the Behavior of Water Reactor Fuel Elements under Accident Conditions, Spatind, Norway, September 1976.

(15) Dobson, W.G., Biederman, R.R., "ZORO-1 - A Finite Difference Computer Model for Zircaloy-4 Oxidation in Steam". EPRI-NP-347, December 1976.

(16) Malang, S., Neitzel, H.J., "Modelling of Zircaloy-Steam-Oxidation under Severe Fuel Damage Conditions". OECD-NEA-CSNI/IAEA Specialists Meeting on Water Reactor Fuel Safety and Fission Product Release in Off-Normal and Accident Conditions, Risø National Laboratory, Denmark, May 1983, Summary Report IWGFPT/16, pp. 213-219.

(17) Suzuki, M., Kawasaki, S., "Development of Computer Code PRECIP-II for Calculations of Zr-Steam Reaction." J. Nucl. Sci. Technol. 17 (1980), pp. 291-300.

(18) Hofmann, P., Neitzel, H.J., "External and Internal Reaction of Zircaloy Tubing with Oxygen and UO_2 and its Modelling." KfK 3880/2, December 1984, pp. 1015-1025.

(19) Sawatzky, A., Ledoux, G.A., Jones, S., "The Oxidation of Zirconium During a High-Temperature Transient". ASTM Conference on Zirconium in the Nuclear Industry, Quebec City, Que, Canada, August 1976.

(20) Leistikow, S., Schanz, G., v. Berg, H., "Investigations into the Temperature-Transient Steam Oxidation of Zircaloy-4 Cladding Material under Hypothetical PWR Loss-of-Coolant Accident Conditions". KfK 2810, April 1979.

(21) Furuta, T., Kawasaki, S., Hashimoto, M., Otomo, T., "Influence of Deformation on the Subsequent Steam Oxidation of Zircaloy Cladding". JAERI-M 6869, December 1976.

(22) Bradhurst, D.H., Heuer, P.M., "The Effects of Deformation on the High-Temperature Steam Oxidation of Zircaloy-2". J. of Nuclear Materials 55 (1975), pp. 311-326.

(23) Leistikow, S., Kraft, S., "Creep Rupture Testing of Zircaloy-4 Tubing under Superimposed High-Temperature Steam Oxidation at 900 °C". Proc. 6th European Congress on Metallic Corrosion, London, September 1977, pp. 577-584.

(24) Hofmann, P., "Über die mechanische Beanspruchung von Zirkonium, Zircaloy und anderen Werkstoffen durch die Bildung von Oxidschichten (Literaturstudie)". KfK Ext. 6/77-2, Juni 1977.

(25) Bocek, M., Petersen, C., "The Influence of Oxide Coatings on the Ductility of Zircaloy-4". J. of Nuclear Materials 80 (1979), pp. 303-313.

(26) Leistikow, S., Kraft, R., Pott, E., "Is Air a Suitable Environment for Simulation of Zircaloy/Steam High-Temperature Oxidation within Engineering Experiments ?" Proc. Europ. Symp. on the Interaction between Corrosion and Mechanical Stress at High Temperatures, Petten, Netherlands, May 1980.

(27) Leistikow, S., Kraft, R., "Kriech-Berst-Untersuchungen zum Kühlmittelverlust-Störfallverhalten von Zircaloy-4-Hüllrohren in Argon und Wasserdampf". Jahrestagung Kerntechnik Hannover, FRG, April 1978, pp. 549-552.

(28) Raff, S., Bocek, M., Meyder, R., "Mechanical Properties of Zircaloy - NORA." Seventh Water Reactor Safety Research Information Meeting, Gaithersburg, MD, USA, November 5-9, 1979.

(29) Chung, H.M., Garde, A.M., Kassner, T.F., "Mechanical Properties of Zircaloy Containing Oxygen". In: Light-Water-Reactor Safety Research Program, Quarterly Progress Report April-June 1975, ANL-75-58, pp. 47-83.

(30) Hofmann, P., Politis, C., "The Kinetics of the Uranium Dioxide-Zircaloy Reactions at High Temperatures". J. of Nuclear Materials 87 (1979), pp. 375-397.

(31) Hofmann, P., Kerwin-Peck, D., "UO_2/Zircaloy-4 Chemical Interactions from 1000 to 1700 °C under Isothermal and Transient Temperature Conditions". J. of Nuclear Materials 124 (1984), pp. 80-105.

(32) Hofmann, P., Spino, J., "Stress Corrosion Cracking of Zircaloy-4 Cladding at Elevated Temperatures and its Relevance to Transient LWR Fuel Rod Behaviour". J. of Nuclear Materials 125 (1984), pp. 85-95.

(33) Furuta, T., Hashimoto, M., Otomo, T., Kawasaki, S., Honma, K., "Deformation and Inner Oxidation of the Fuel Rod in a Loss-of-Coolant Accident Condition." JAERI-M 6339, November 1975.

(34) Furuta, T., Uetsuka, H., Kawasaki, S., Hashimoto, M., Otomo, T., "Extent of Oxide Layer at the Inner Surface of Burst Cladding". JAERI-M 9475, April 1981.

(35) Furuta, T., Kawasaki, S., "Reaction Behaviour of Zircaloy-4 in Steam Hydrogen Mixtures at High Temperature". J. of Nuclear Materials 105 (1982), pp. 119-131.

(36) Karb, E.H., Prüssmann, M., Sepold, L., Hofmann, P., Schanz, G., "LWR Fuel Rod Behaviour in the FR2 In-pile Tests Simulating the Heatup Phase of a LOCA, Final Report". KfK 3346, March 1983.

(37) Hofmann, P., Petersen, C., Schanz, G., Zimmermann, H., "In-pile Experimente zum Brennstabverhalten beim Kühlmittelverluststörfall. Ergebnisse der zerstörenden Nachuntersuchungen der Versuchsserie G (35000 MWd/t_U)". KfK 3433, Juni 1983.

(38) Uetsuka, H., Furuta, T., Kawasaki, S., "Zircaloy-4 Cladding Embrittlement due to Inner Surface Oxidation under Simulated Loss-of-Coolant Condition". J. of Nuclear Science and Technology 18 (1981), pp. 705-717.

(39) Uetsuka, H., Furuta, T., Kawasaki, S., "Zircaloy Cladding Embrittlement due to Inner Surface Oxidation During a LOCA - Inner Surface Oxidation Experiment using a Simulated Fuel Rod (2) - Influences of UO_2-Steam Reaction and Rapid Cooling". JAERI-M 9681, August 1981.

(40) Hobson, D.O., Rittenhouse, P.L., "Embrittlement of Zircaloy-Clad Fuel Rods by Steam During LOCA Transients". ORNL 4758, January 1972.

(41) Furuta, T.M Uetsuka, H.; Kawasaki, S.: "Estimation of Conservatism of Present Embrittlement Criteria for Zircaloy Fuel Cladding under LOCA". Proc. 6th Intern. Symp. "Zirconium in the Nuclear Industry" Vancouver, BC, Canada (1982), pp. 734-746.

(42) Pawel, R.E., "Oxygen Diffusion in Beta Zircaloy during Steam Oxidation". J. of Nuclear Materials 50 (1974), pp. 247-258.

(43) Chung, H.M., Kassner, T.F., "Embrittlement Criteria for Zircaloy Fuel Cladding applicable to Accident Situations in Light-Water-Reactors". Summary Report". NUREG/CR-1344, January 1980.

(44) Haggag, F.M., "Zircaloy Cladding Embrittlement Criteria: Comparison of In-Pile and Out-of-Pile Results". NUREG/CR-2757, EGG-2123, R3, July 1982.

(45) Busby, C.C., Marsh, K.B., "High Temperature Deformation and Burst Characteristics of Recrystallized Zircaloy-4 Tubing", WAPD-TM-900, January 1970.

(46) Hobson, D.O., Rittenhouse, P.L., "Deformation and Rupture Behavior of Light Water Reactor Fuel Cladding". ORNL-4727, October 1971.

(47) Hardy, D.G., "High Temperature Expansion and Rupture Behavior of Zircaloy Tubing". Proceedings of ANS Topical Meeting on Water Reactor Safety, March 1973, Salt Lake City, UT, USA.
CONF-730 304. pp. 254-273.

(48) Chapman, R.H., "Multirod Burst Test Program, Quarterly Progress Report for April-June 1977". ORNL/NUREG/TM-135, December 1977.

(49) Chung, H.M., Kassner, T.F., "Deformation Characteristics of Zircaloy Cladding in Vacuum and Steam under Transient-Heating Conditions: Summary Report", NUREG/CR-0344, July 1978.

(50) Burman, D.L. et al., "Comparison of Westinghouse LOCA Burst Test Results with ORNL and other Program Results". Proceedings of a CSNI Specialist Meeting on Safety Aspects of Fuel Behavior in Off-normal and Accident Conditions, Espoo, Finland, September 1980. pp. 251-284.

(51) Mac Donald P.E. et al., "Cladding Deformation during a Large Break LOCA". ANS-ENS Topical Meeting on Reactor Safety Aspects of Fuel Behavior, August 1981, Sun Valley, ID, USA.

(52) Furuta, T., et al., "Zircaloy-Clad Fuel Rod Burst Behavior under Simulated Loss-of-Coolant Condition in Pressurized Water Reactors". Journal of Nuclear Science and Technology, 15 /10/, October 1978, pp. 736-744.

(53) Hindle, E.D., "Zircaloy Fuel Clad Ballooning Tests at 900-1070 K in Steam", ND-R-6 (s) June 1977, 1st Supplement, October 1977.

(54) Hindle, E.D., Mann, C.A., "An Experimental Study of the Deformation of Zircaloy PWR Fuel Rod Cladding under Mainly Convective Cooling", Proceedings of the Fifth International Conference on Zirconium in the Nuclear Industry, Boston, MA, USA, August 1980, ASTM-STP 754, pp. 284-302.

(55) Morize, P. et al., "Zircaloy Cladding Diametral Expansion during a LOCA, EDGAR programme". CSNI Proceedings of Specialist Meeting on the Behavior of Water Reactor Fuel Elements under Accident Conditions, INIS-MF-3224, Spatind, Norway, September 1976, pp. 30-31.

(56) Jones, P. et al., "EOLO-JR: A Single Rod Burst Test Program in the ESSOR Reactor", ANS-ENS Topical Meeting on Reactor Safety Aspects of Fuel Behavior, August 1981, Sun Valley, ID, USA.

(57) Cheliotis, G. et al., "Verification of LOCA Clad Ballooning Behavior in

Multi-Rod Tests by Means of Single Rod Investigations". Proceedings of a CSNI Specialist Meeting on Safety Aspects of Fuel Behaviour in Off-Normal and Accident Conditions, Espoo, Finland, September 1980, pp. 111-140.

(58) Lehning, H. et al., "Berstversuche an Zircaloy-Hüllrohren unter kombinierter mechanisch-chemischer Beanspruchung (FABIOLA)". Jahrestagung Kerntechnik, Berlin, März 1980, pp. 231-234.

(59) Bocek, M. et al., "Verification of Life Time Predictions by Means of Temperature-Transient Burst Tests on Zry-4 Fuel Rod Simulators". Proceedings of a CSNI Specialist Meeting on Safety Aspects of Fuel Behavior in Off-Normal and Accident Conditions, Espoo, Finland, September, 1980, pp. 223-237.

(60) Hofmann, P., Raff, S., "Verformungsverhalten von Zircaloy-4-Hüllrohren unter Schutzgas im Temperaturbereich zwischen 600 und 1200 °C". KfK 3168, Juli 1981.

(61) Erbacher, F. et al., "Out-of-pile Experiments on Ballooning in Zircaloy Fuel Rod Claddings in the Low Pressure Phase of a Loss-of-Coolant Accident". Proceedings of the Specialist Meeting on the Behavior of Water Reactor Fuel Elements under Accident Conditions, Spatind, Norway, September 1976.

(62) Erbacher, F., Neitzel, H.J., Wiehr, K., "Studies on Zircaloy Fuel Clad Ballooning in a Loss-of-Coolant Accident - Results of Burst Tests with Indirectly Heated Fuel Rod Simulators". Proceedings of the Fourth International Conference on Zirconium in the Nuclear Industry, Stratford-upon-Avon, England, June 1978, ASTM-STP 681, pp. 429-446.

(63) Erbacher, F.J. et al., "Burst Criterion of Zircaloy Fuel Claddings in a Loss-of-Coolant Accident". Proceedings of the Fifth International Conference on Zirconium in the Nuclear Industry, Boston, MA, USA, August 1980, ASTM-STP 754, pp. 271-283.

(64) Neitzel, H.J., Rosinger, H.E., "The Development of a Burst Criterion for Zircaloy Fuel Cladding under LOCA Conditions". KfK 2893, AECL-6420,

October 1980.

(65) Kawasaki, S., "Multirod Burst Tests under Loss-of-Coolant Conditions". OECD-NEA-CSN/IAEA-Specialists` Meeting on Water Reactor Fuel Safety and Fission Product Release in Off-Normal and Accident Conditions, May 1983, Risø National Laboratory, Denmark.

(66) Chapman, R.H. et al., "Effect of Bundle Size on Cladding Deformation in LOCA Simulation Tests". Sixth International Conference on Zirconium in the Nuclear Industry, June/July 1982, Vancouver, BC, Canada.

(67) Cheliotis, G., Ortlieb, E., "Parameteruntersuchungen über die Beeinflussung der Hüllrohre durch Nachbarstäbe beim Kühlmittelverluststörfall". Abschlußbericht Förderungsvorhaben BMFT RS 185 A, KWU Bericht R 914/022/80, September 1980.

(68) Adroguer, B., Hueber, C., Trotabas, M., "Behavior of PWR Fuel in LOCA Conditions, PHEBUS Test 215 P". OECD-NEA-CSNI/IAEA Specialists` Meeting on Water Reactor Fuel Safety and Fission Product Release in Off-Normal and Accident Conditions, May 1983, Risø National Laboratory, Denmark.

(69) Mohr, C.L. et al., "LOCA Simulation in the National Research Universal Reactor Program, Third Materials Experiment (MT-3)". NUREG/CR-2528, PNL-4166, April 1983.

(70) Wiehr, K. et al., KfK 3450, Juni 1984, pp. 4200-42 bis -96.

(71) Wiehr, K. et al., KfK 3350, Juli 1983, pp. 4200-94 bis -162.

(72) Wiehr, K. et al., KfK 2700, November 1978, pp. 4200-103 bis -120.

(73) Wiehr, K. et al., KfK 2750, Oktober 1979, pp. 4200-109 bis -144.

(74) Wiehr, K., Juli 1979 (unpublished)

(75) Wiehr, K., Erbacher, F.J., Neitzel, H.J., "Influence of a Cold Control Rod Guide Thimble on the Ballooning Behavior of Zircaloy Claddings in a

LOCA". Proceedings of a CSNI Specialist Meeting on Safety Aspects of Fuel Behavior in Off-Normal and Accident Conditions, Espoo, Finland, September 1980. pp.141-154.

(76) Wiehr, K. et al., KfK 3250, Juni 1982. pp. 4200-90 bis -121.

(77) Loftus, M.J. et al., "PWR FLECHT-SEASET, 21-Rod Bundle Flow Blockage Task, Data and Analysis Report". NUREG/CR-2444, EPRI NP-2014, WCAP-9992, Vol. 1 and 2, September 1982.

(78) Adachi, H. et al., "SCTF Core I Reflooding Test Results". NUREG/CP-0041, Vol 1, p. 287, January 1983.

(79) Pearson, K.G., Cooper, L.A., "Reflood Heat Transfer in Severely Blocked Fuel Assemblies", NUREG/CP-0060, December 1984, pp. 643-672.

(80) Ihle, P., Rust, K., "FEBA-Flooding Experiments with Blocked Arrays, Evaluation Report", KfK-3657, March 1984.

(81) Murao, Y. et al., "Findings in CCTF Core I Test", NUREG/CP-0041, Vol. 1, p. 275, January 1983.

(82) Erbacher, F.J., Ihle, P., Wiehr, K., Müller, U., "Reflood Heat Transfer in PWR Rod Bundles Deformed in a LOCA". International Symposium on Heat Transfer, October 1985, Beijing, China.

(83) Erbacher, F.J., Ihle, P., Rust, K., Wiehr, K., "Temperature and Quenching Behavior of Undeformed, Ballooned and Burst Fuel Rods in a LOCA", KfK 3880/1, December 1984.

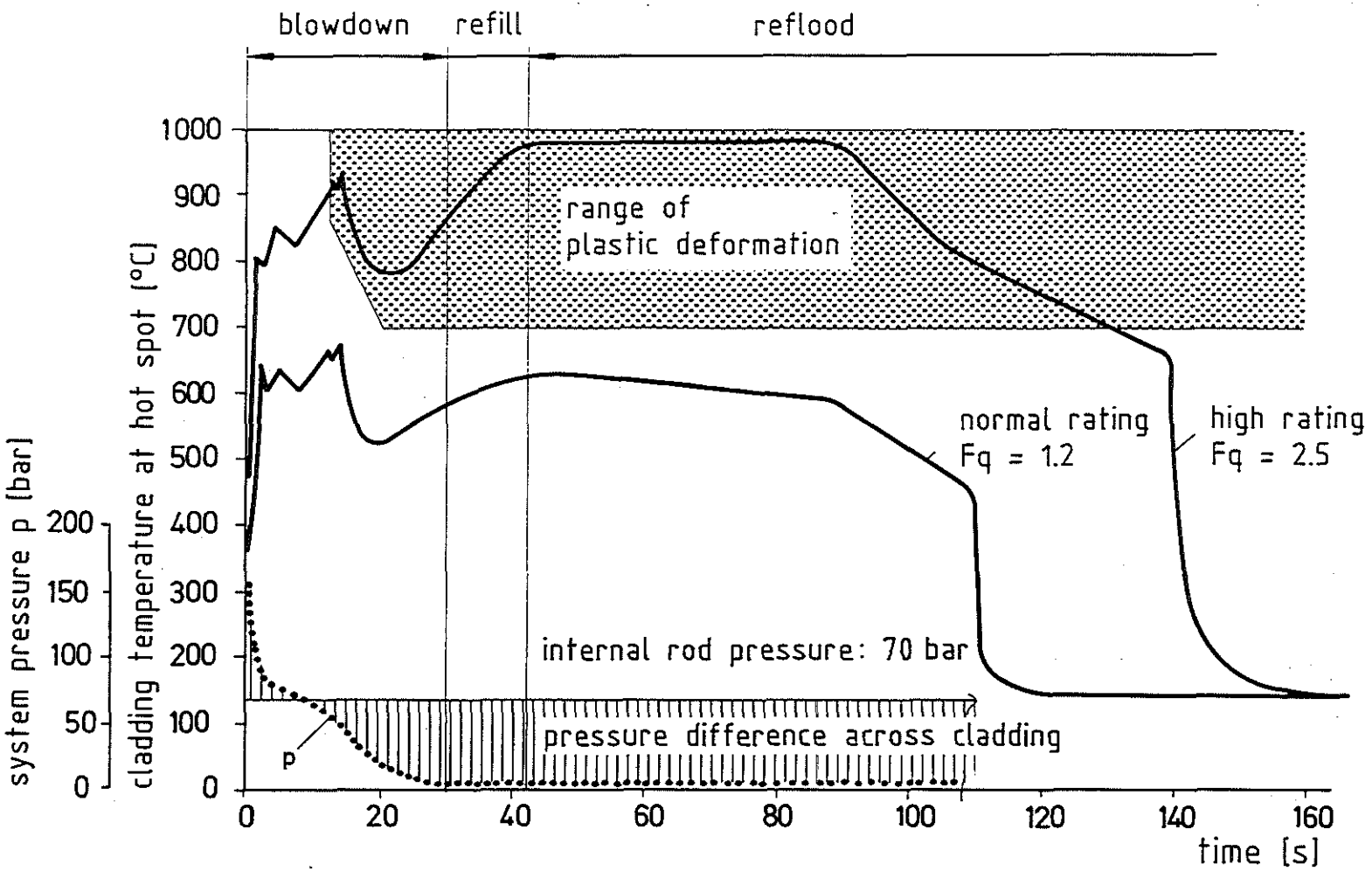

FIG. 1 - Zircaloy-4 fuel rod cladding load in a double-ended cold leg break LOCA

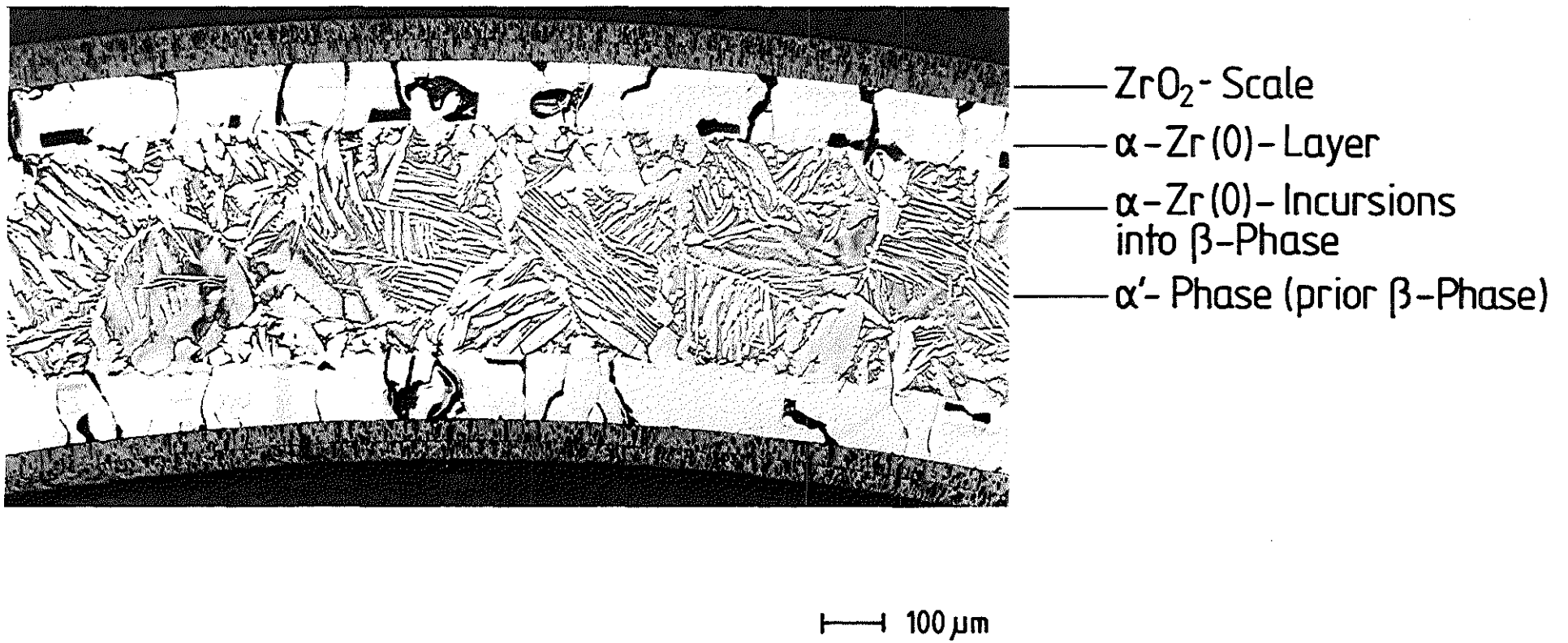

FIG. 2 - Metallographic cross-section of Zircaloy-4 tube wall after double-sided steam oxidation (2 min, 1400 °C)

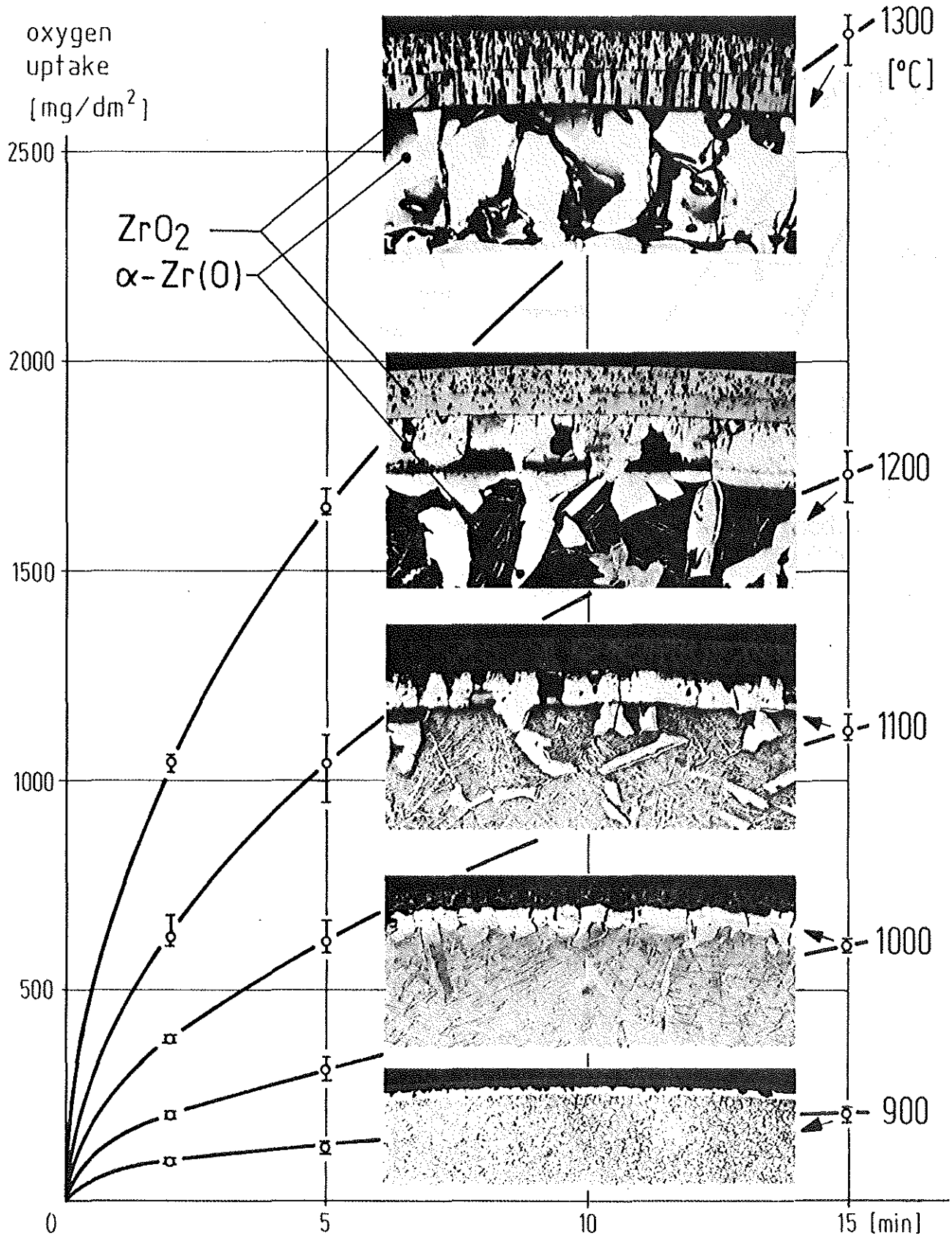

FIG. 3 - Isothermal Zircaloy-4 high temperature steam oxidation:
Mass increase versus time of exposure

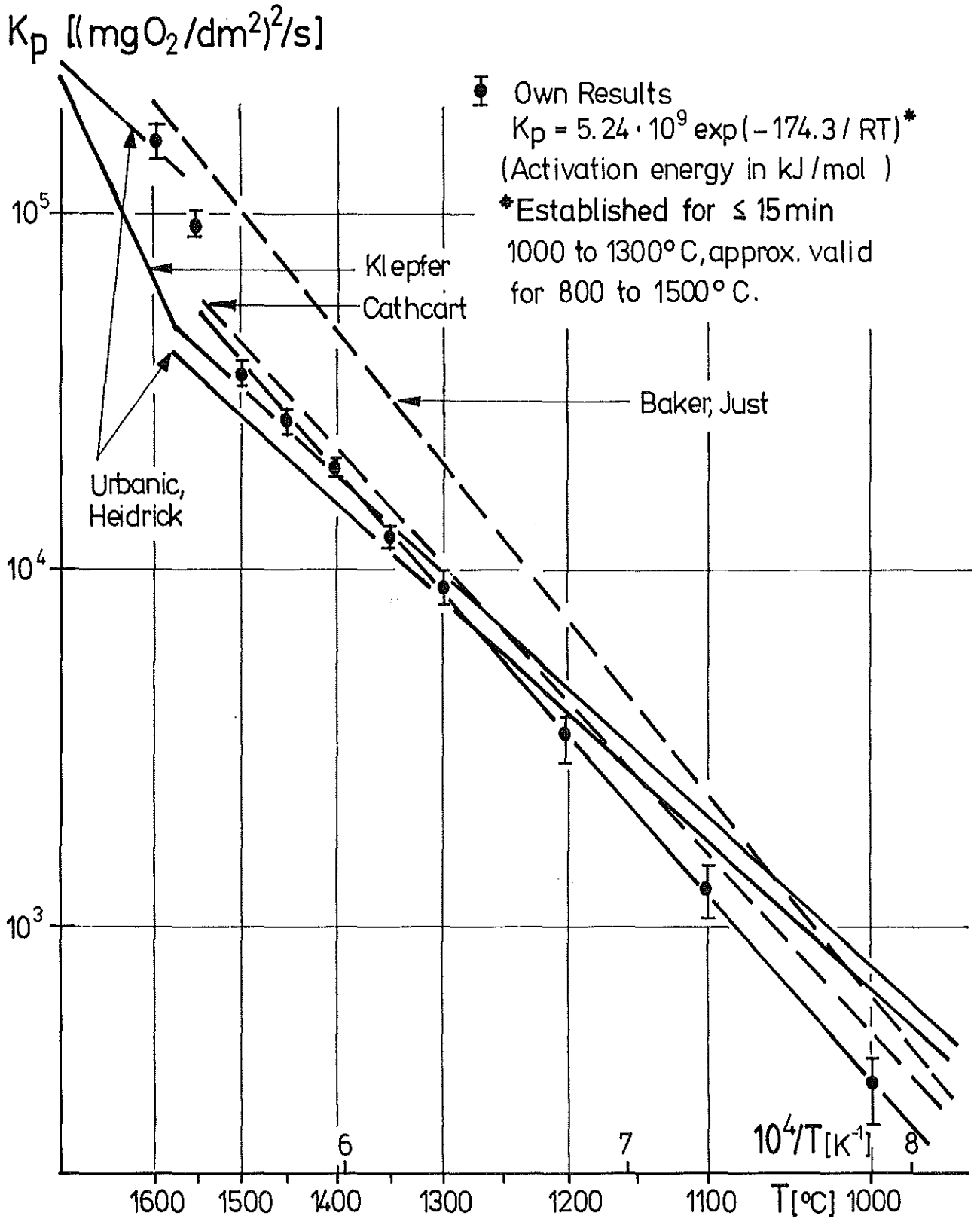

FIG. 4 - Zircaloy-4 high temperature steam oxidation: Parabolic rate constant versus reaction temperature

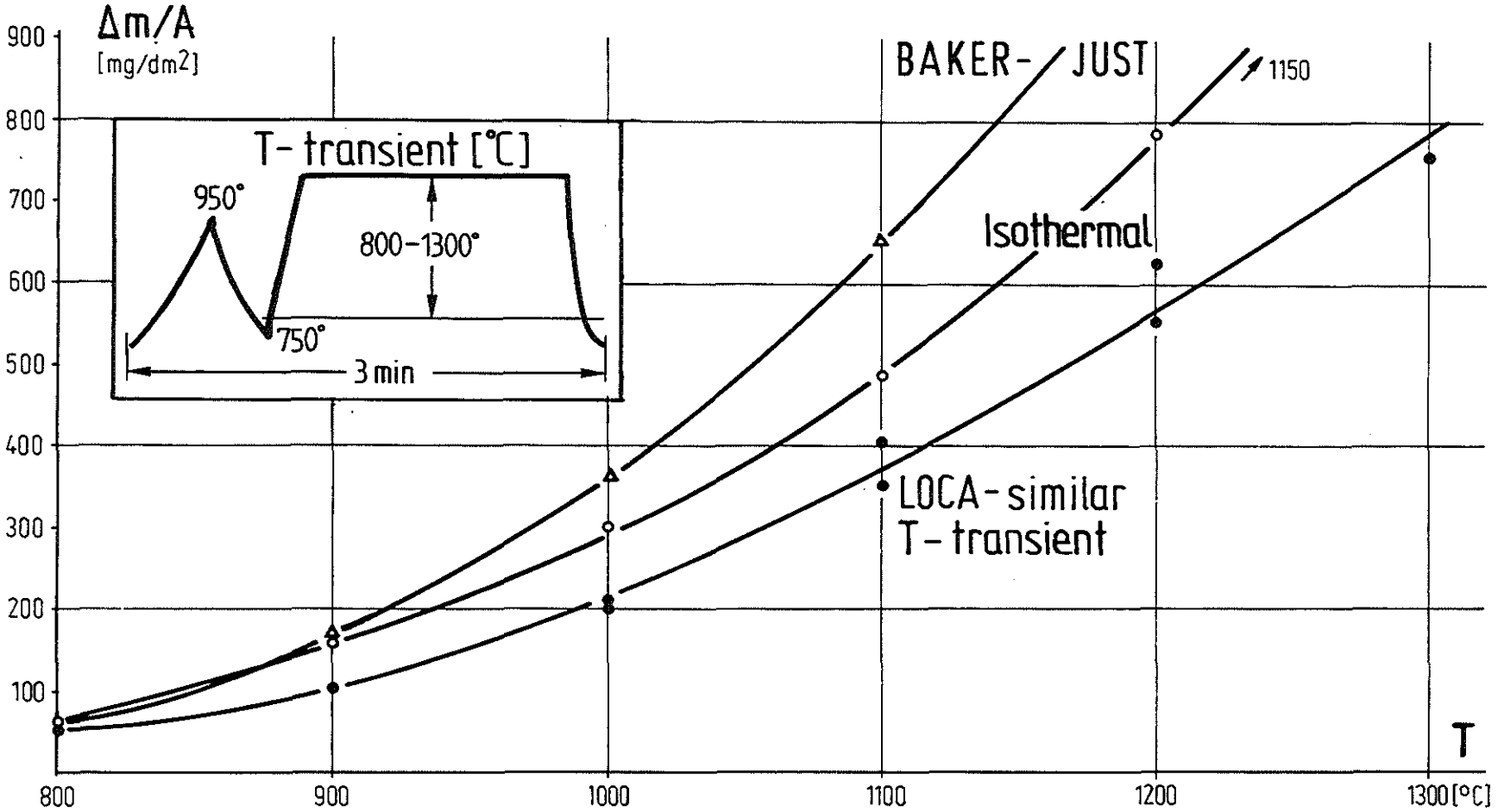

FIG. 5 - Temperature-transient Zircaloy-4 high temperature steam oxidation: Comparison of mass increase during LOCA-similar transients with those of isothermal exposure and as calculated by Baker-Just equation.

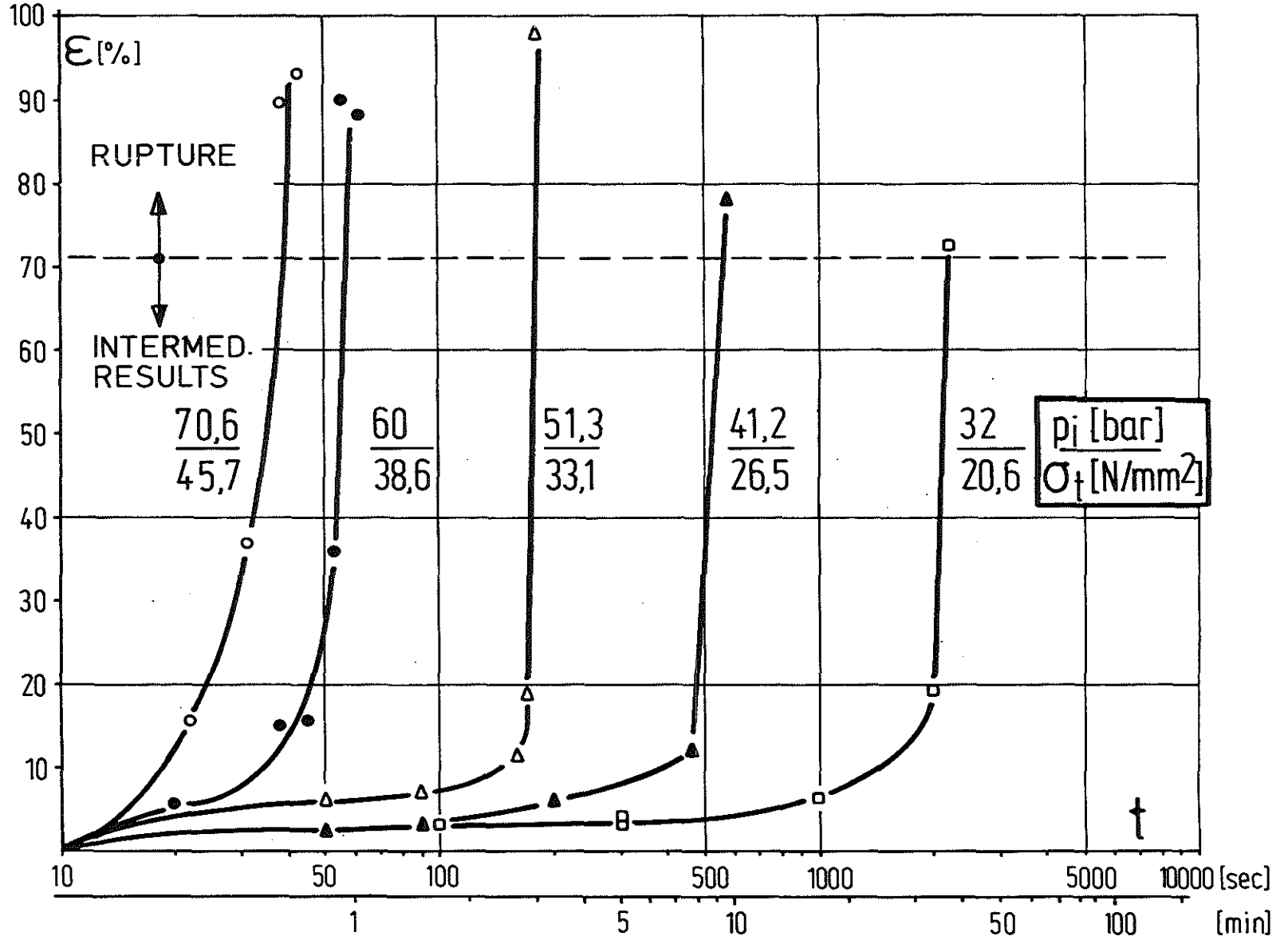

FIG. 6 - Isothermal/isobaric creep curves of Zircaloy-4 tube capsules at 800 °C in steam

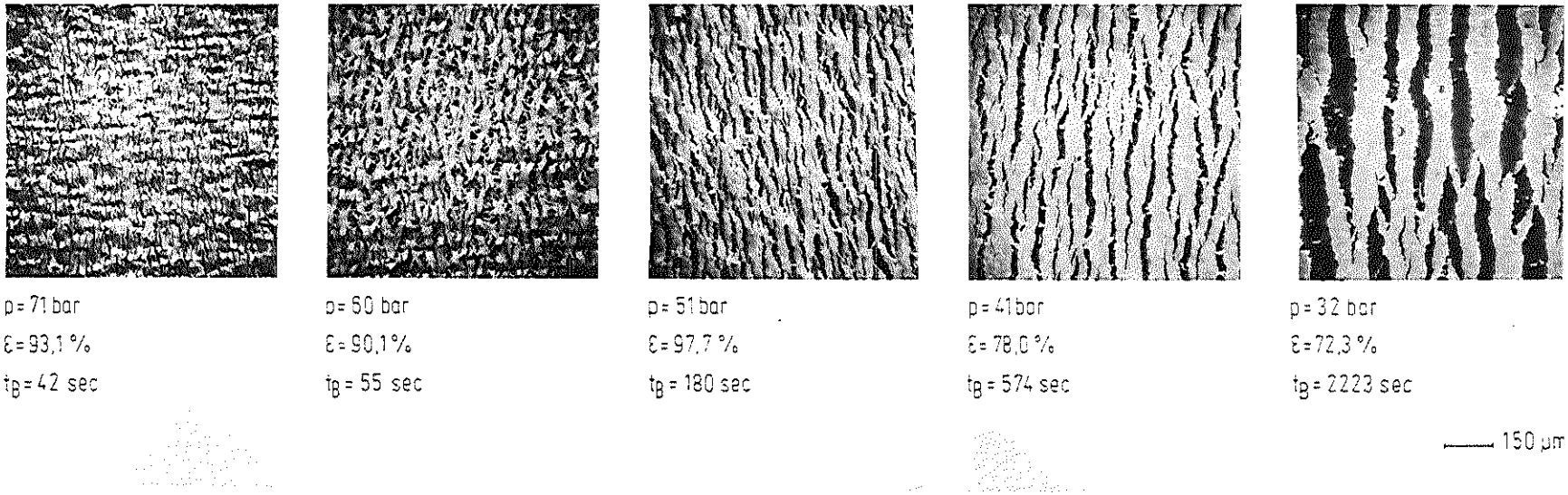

FIG. 7 – Crack pattern of oxidized Zircaloy-4 tube capsule surfaces after creep-rupture tests at 800 °C in steam

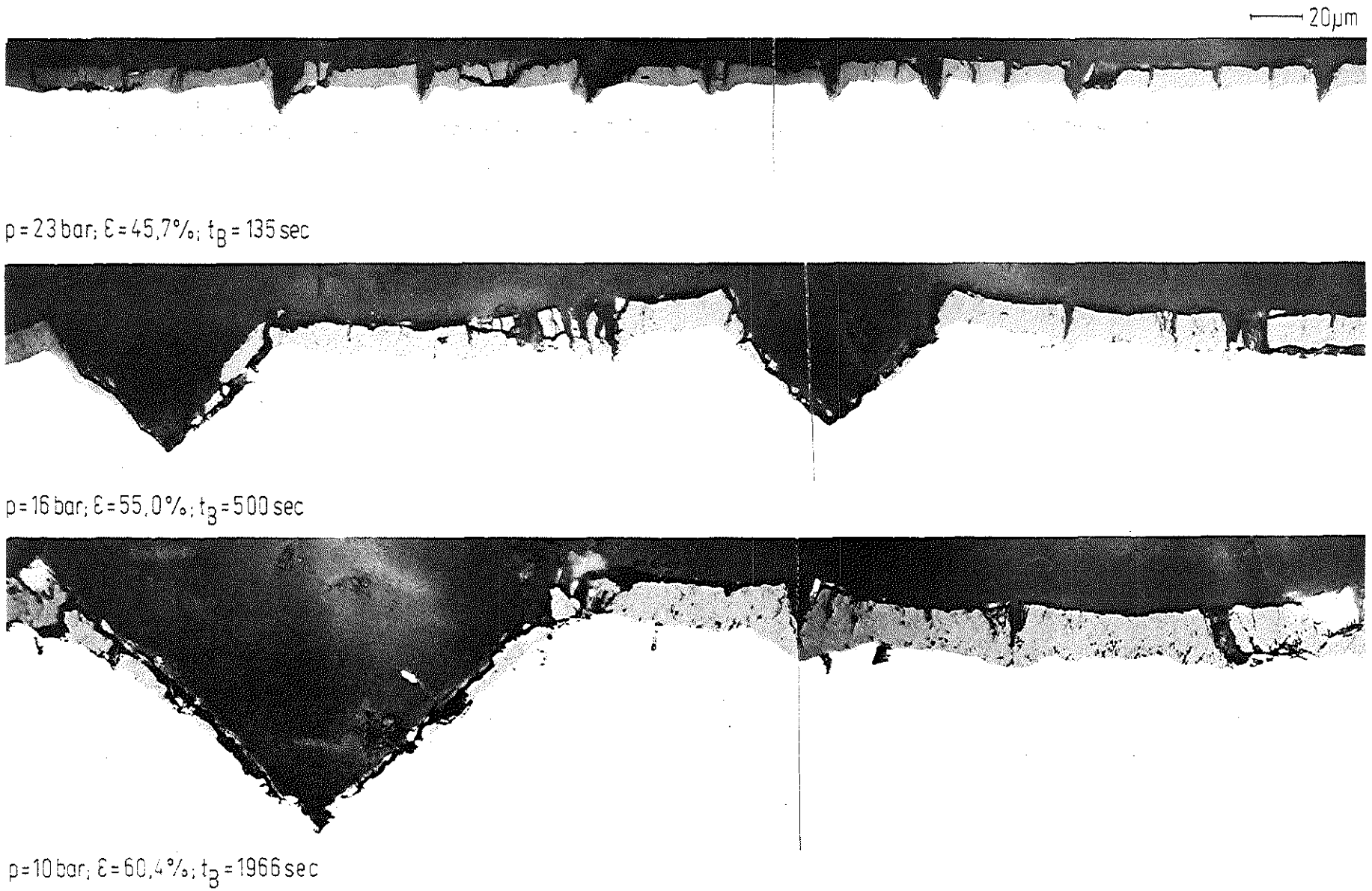

FIG. 8 - Metallographic cross-sections of creep-ruptured Zircaloy-4 tube capsules at 900 °C in steam

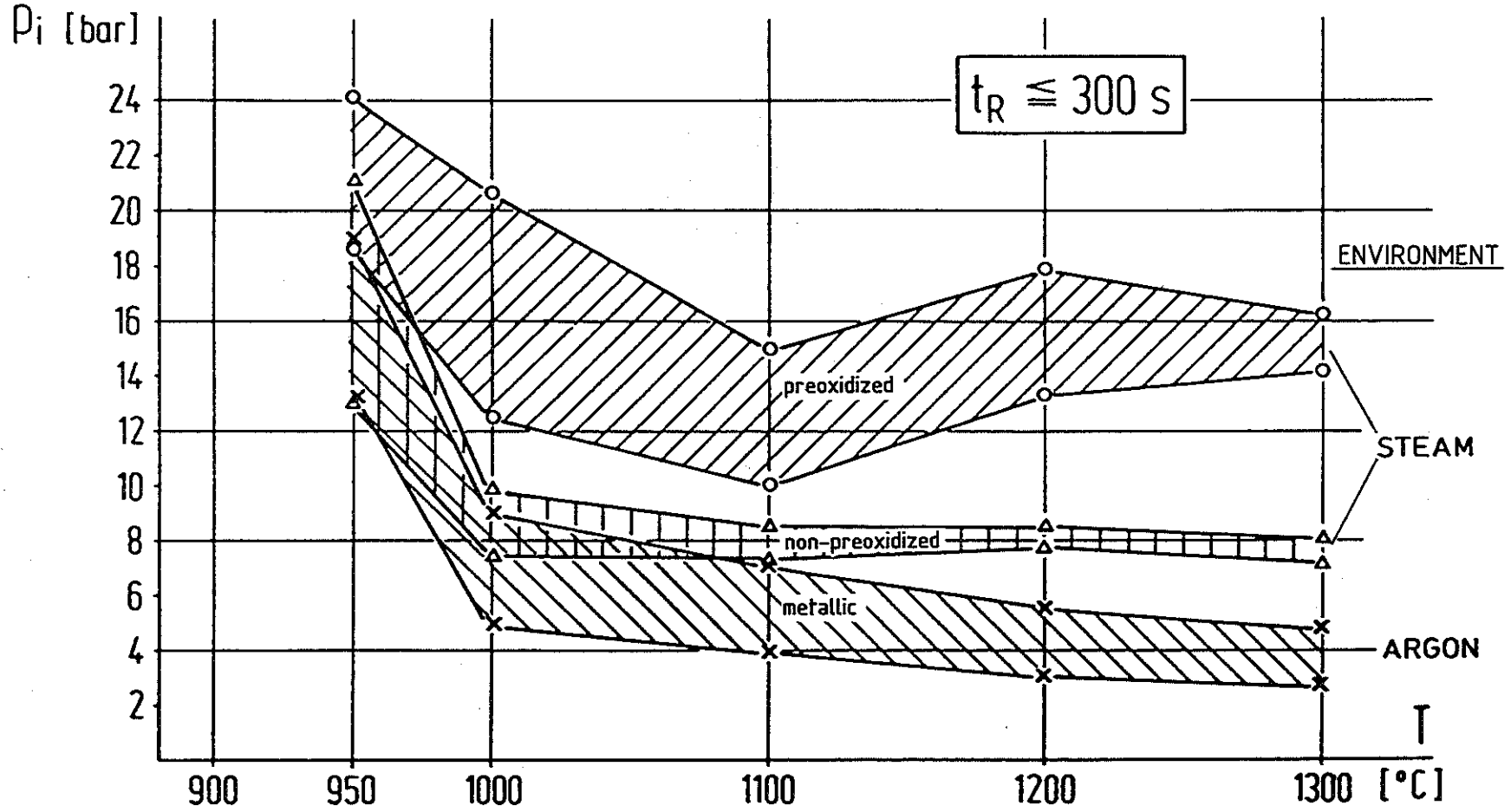

FIG. 9 - Isothermal/isobaric Zircaloy-4 tube capsule tests: Burst pressure versus temperature

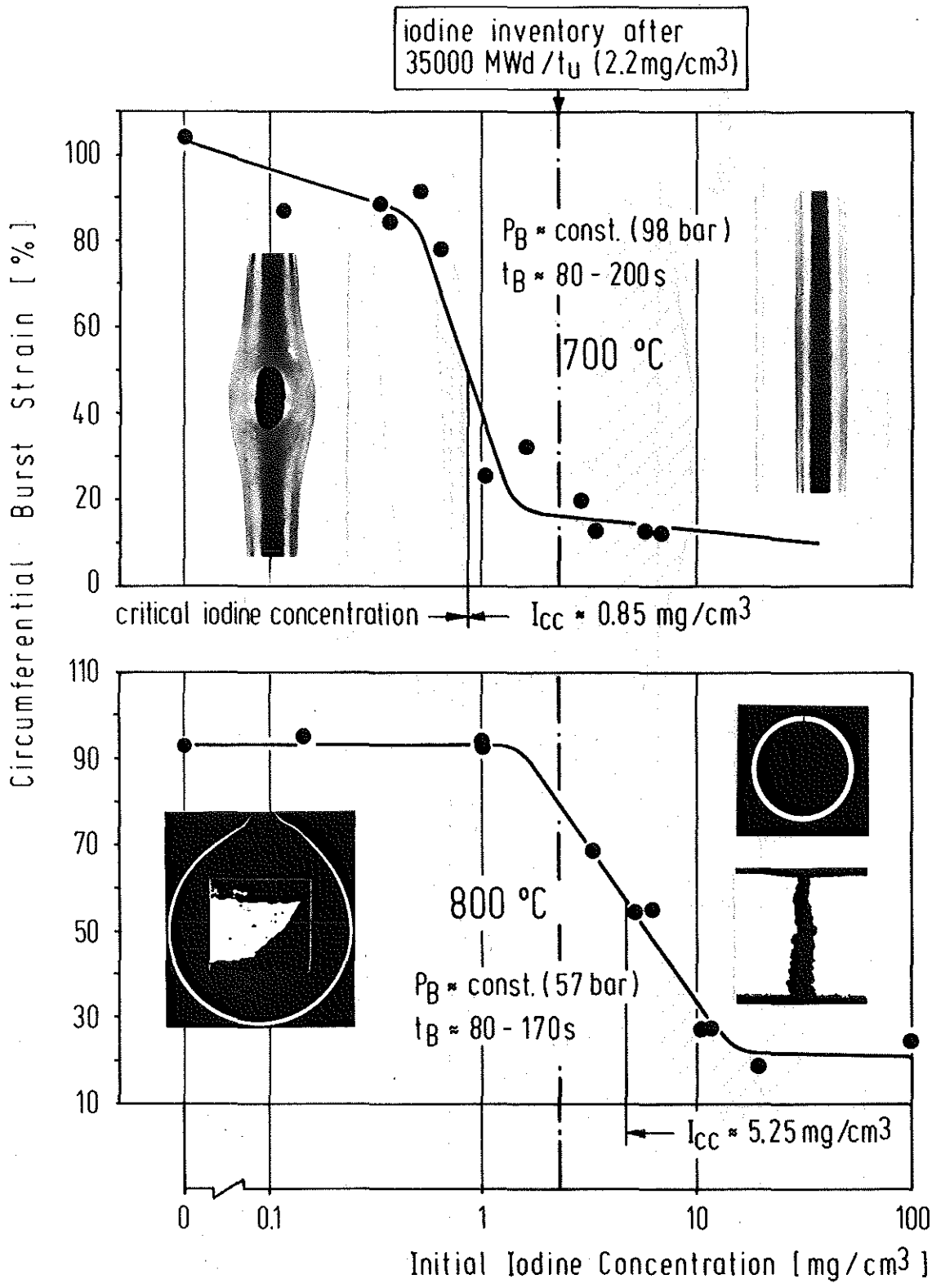

FIG. 10 - Influence of the initial iodine concentration on burst strain of as-received Zircaloy-4 tubing at 700 and 800 °C in the absence of UO_2 fuel.

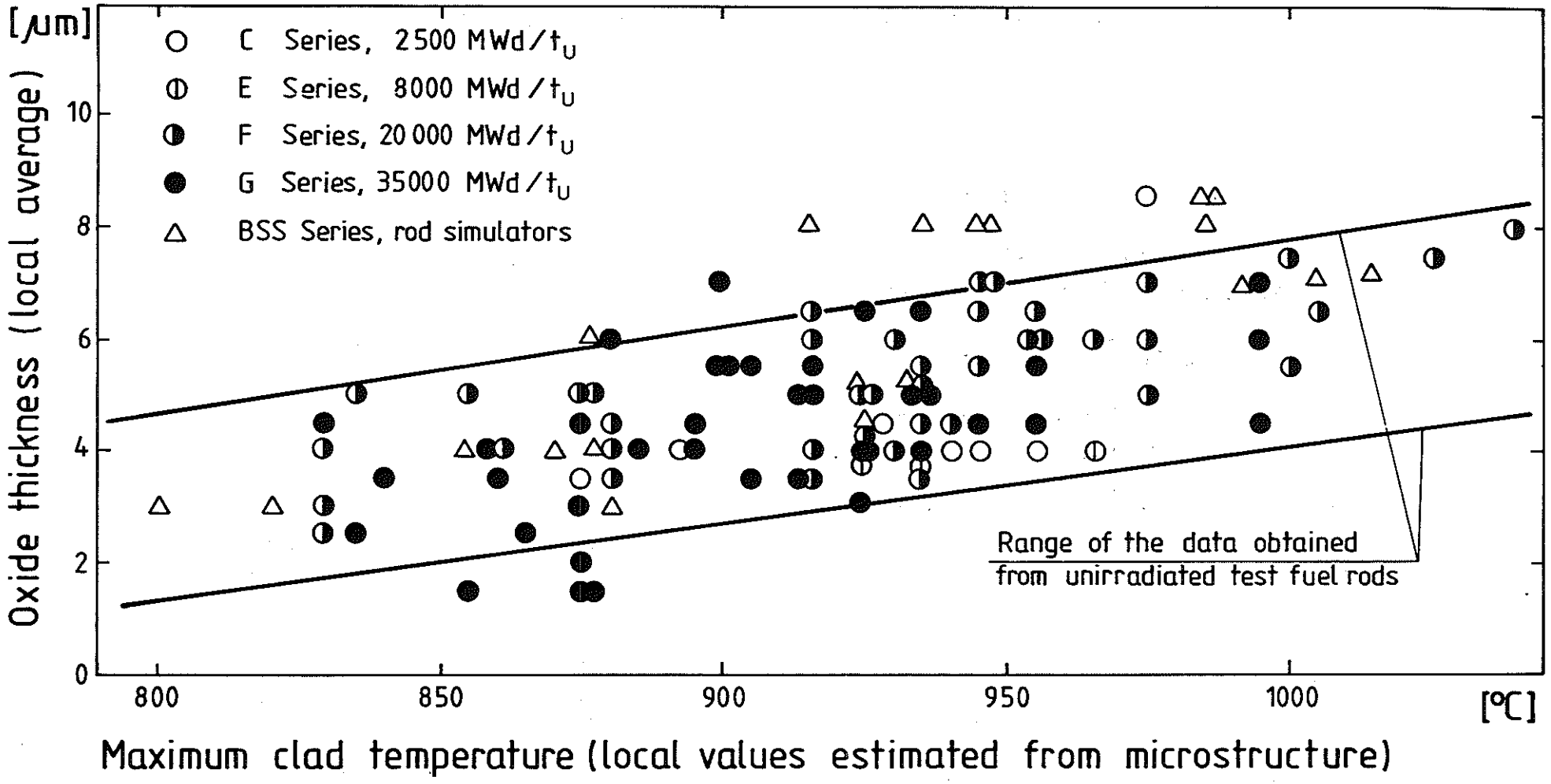

FIG. 11 - FR-2 in-pile tests: Steam oxidation of the cladding outer surface

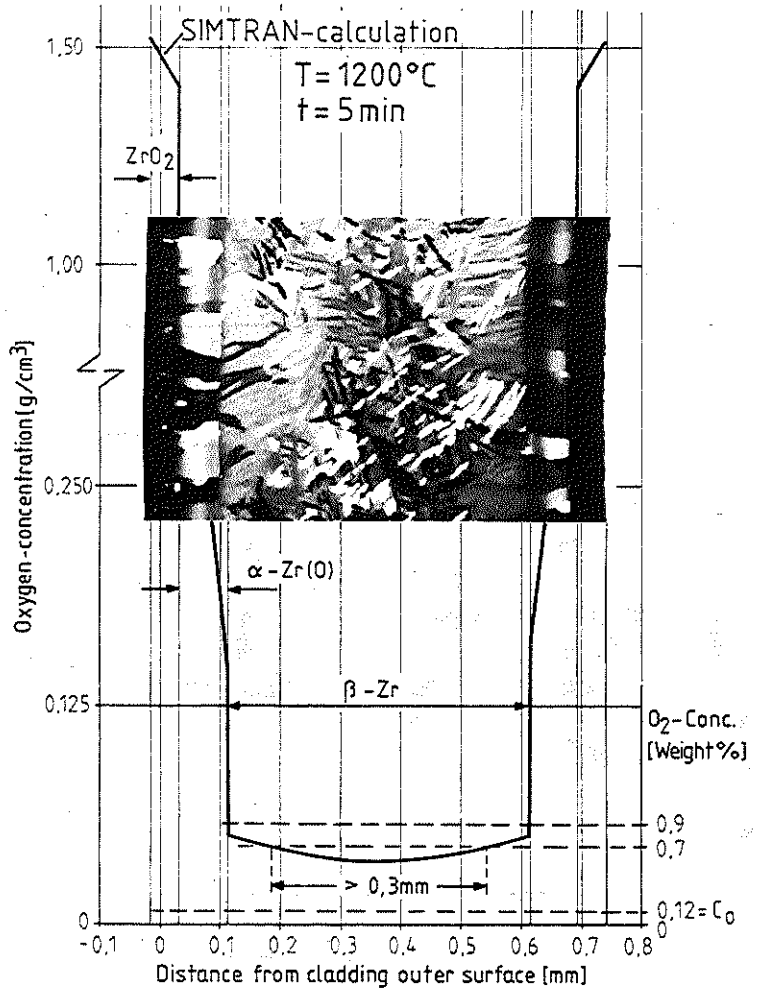

A - At present valid embrittlement criterion:

Limitation of max. cladding temperature and of max. consumption of cladding wall by oxidation

$$T_{max} \leq 1200\ °C$$

$$s_{Zr(+O_2\,total} \xrightarrow{calc.} ZrO_2) \leq 17\%\, s_{wall}$$

B - Proposition of ANL:

Establishment of remaining ductile wall thickness

- with respect to stresses due to thermo-shocks during quenching:

$$s_{0,9\,Weight\%\,O_2} > 0,1\ mm$$

- with respect to handling, transport, interme-diate storage of fuel elements:

$$s_{0,7\,Weight\%\,O_2} > 0,3\ mm$$

FIG. 12 - Penetration and embrittlement of Zircaloy-4 cladding tubes by steam oxidation: Criteria of embrittlement

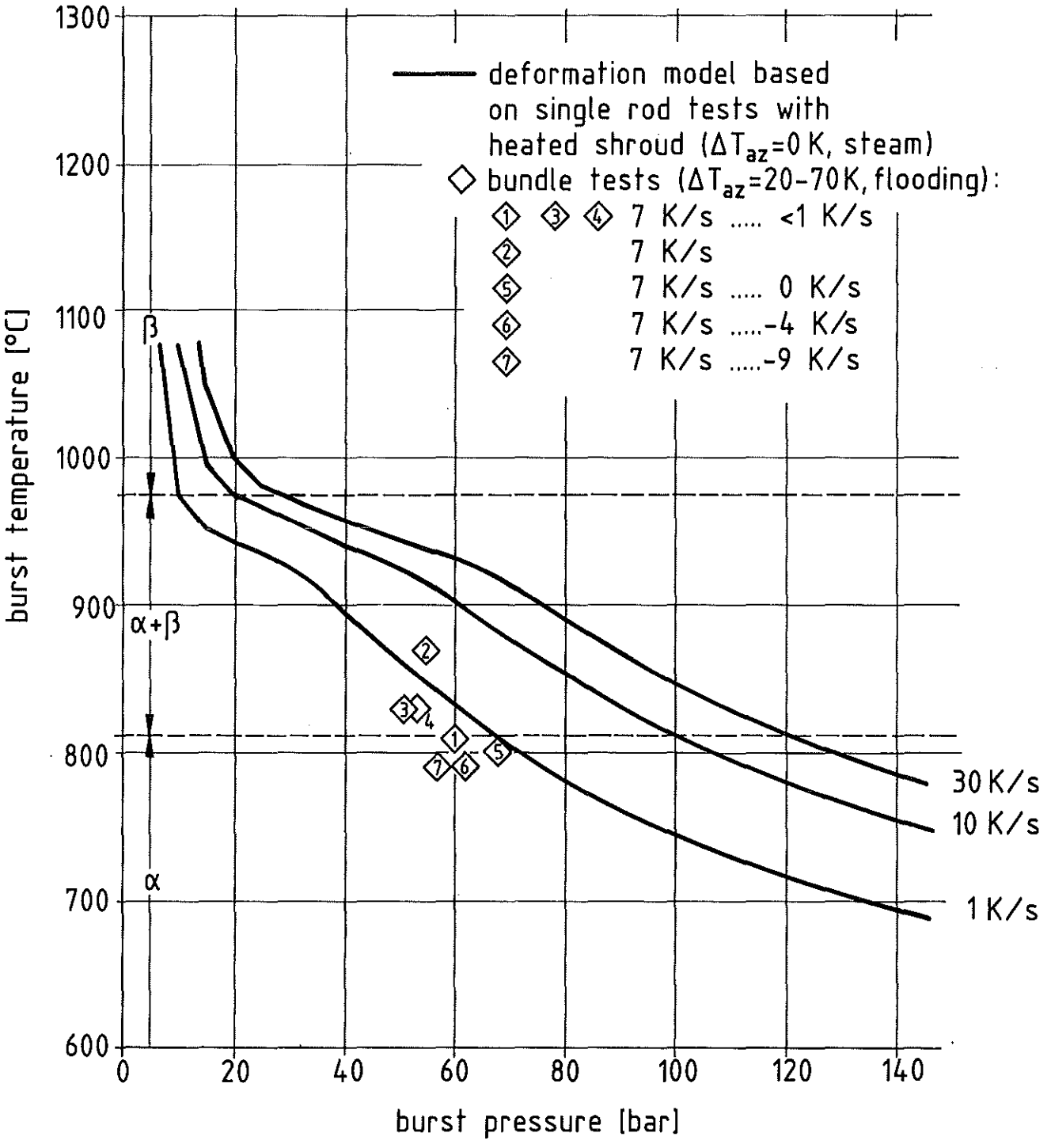

FIG. 13 - Burst temperature versus burst pressure of Zircaloy-4 cladding tubes (REBEKA tests)

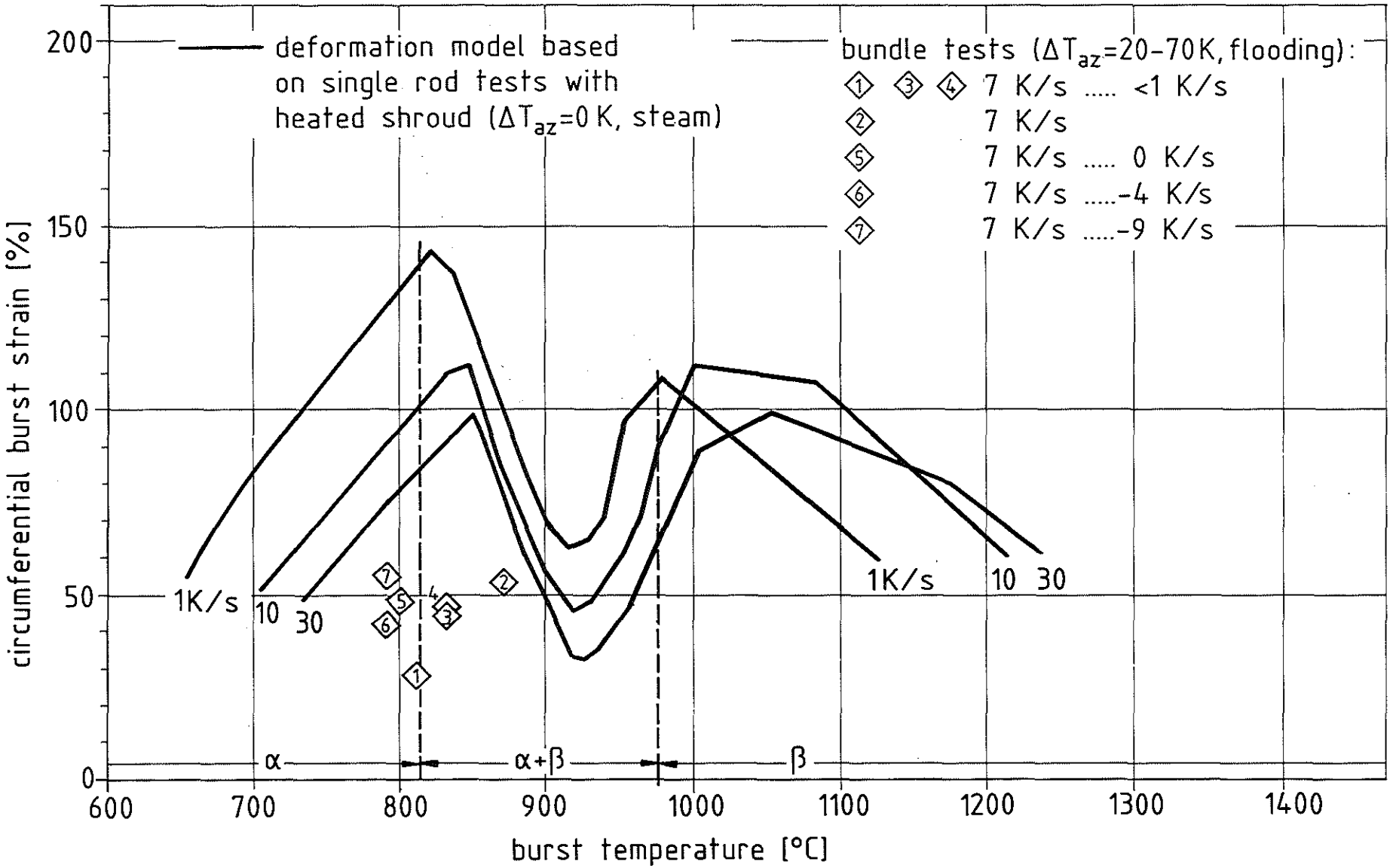

FIG. 14 - Burst strain versus burst temperature of Zircaloy-4 cladding tubes (REBEKA tests)

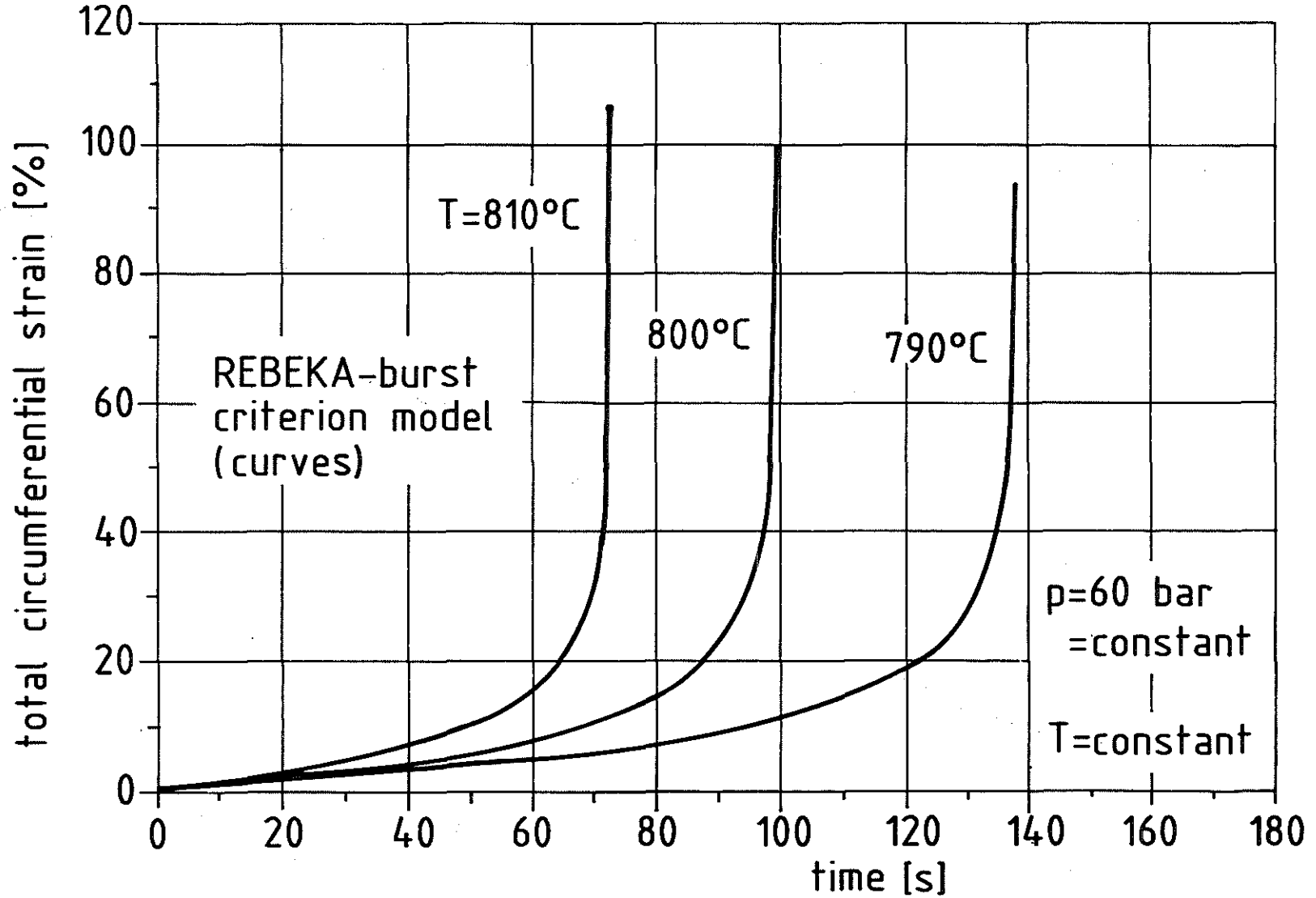

FIG. 15 - Sensitivity of Zircaloy-4 deformation to temperature

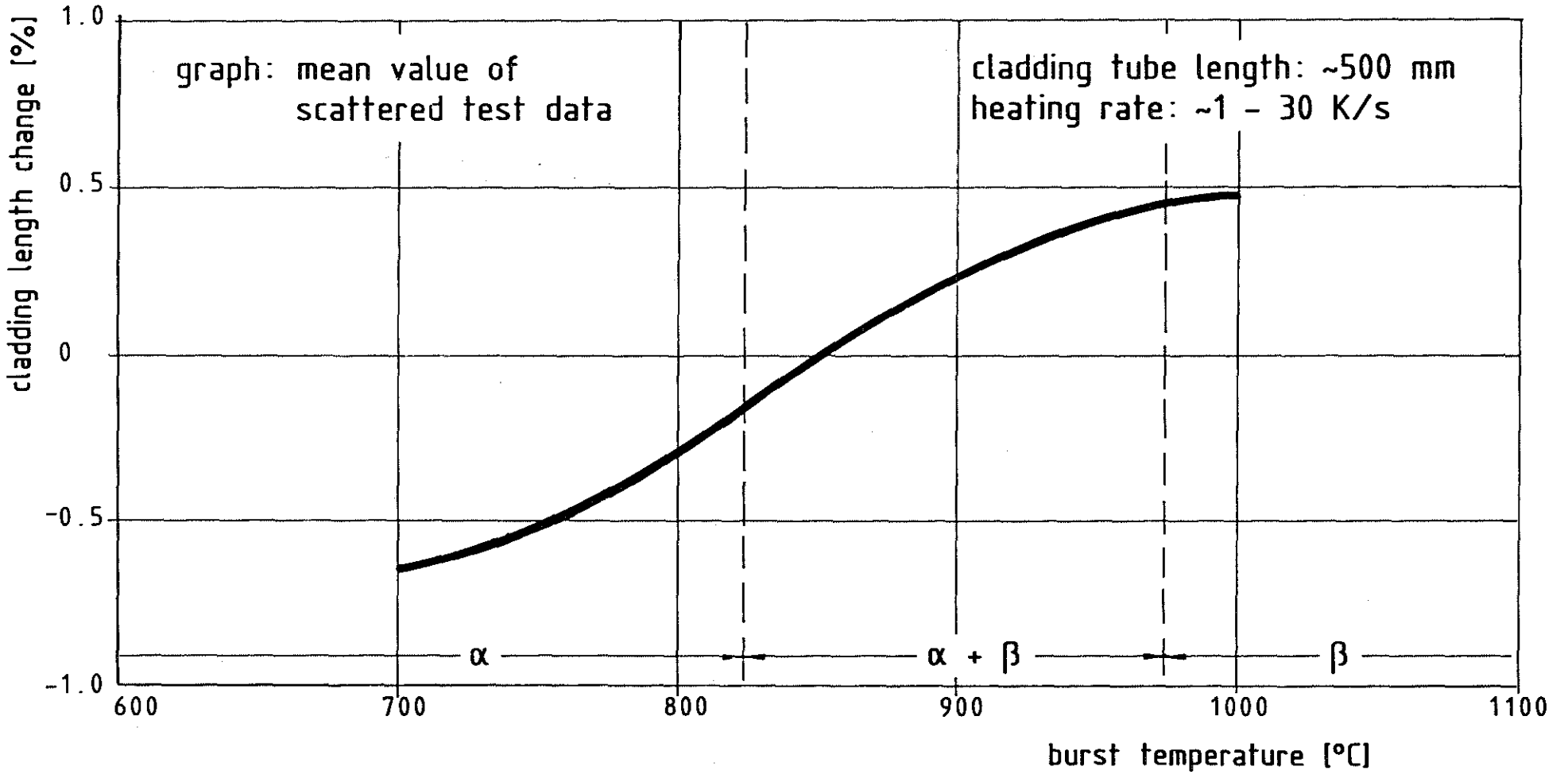

FIG. 16 - Zircaloy-4 cladding tube length change versus burst temperature (REBEKA tests)

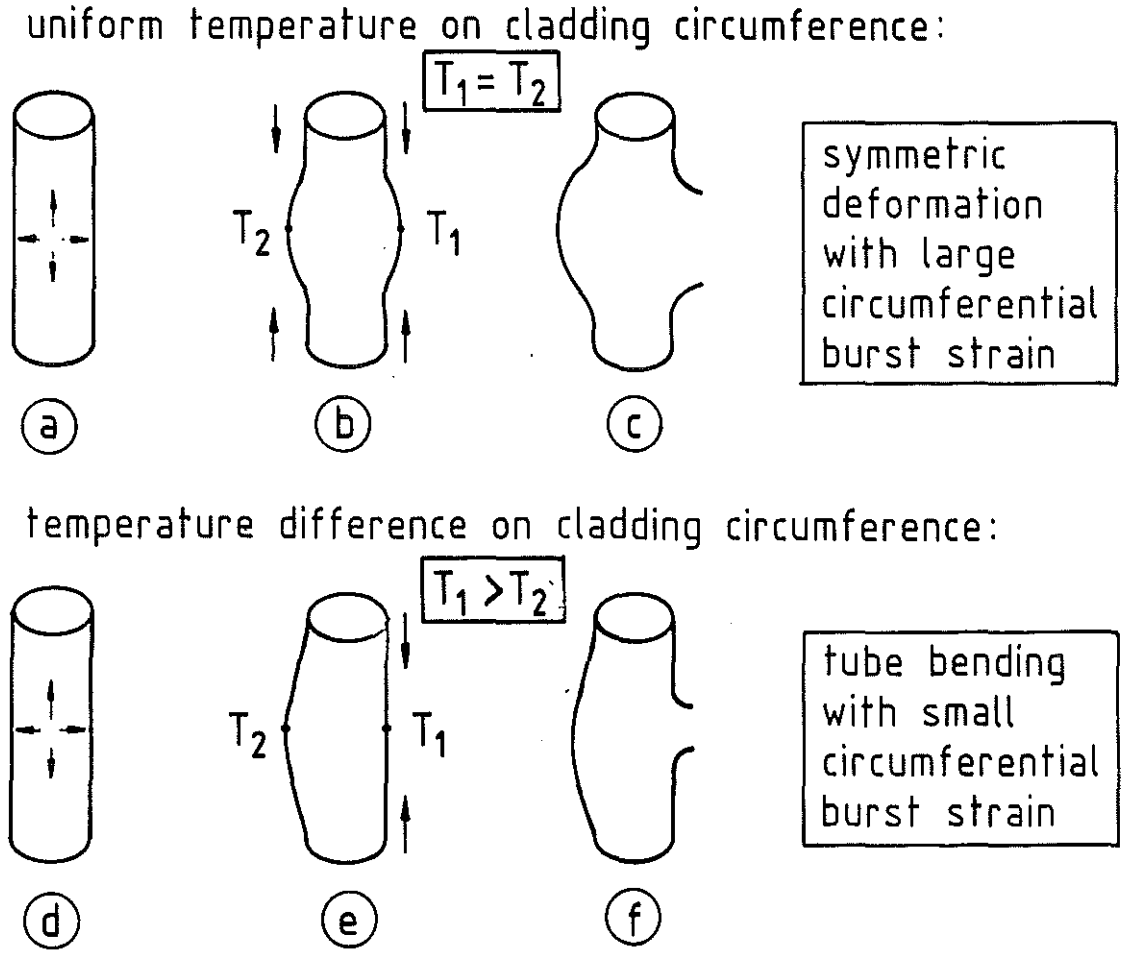

(a) (d) tube under biaxial stress due to internal gas overpressure

(b) axial material flow and tube shortening

(e) hot side:
axial material flow, tube shortening, cladding contacts inner heat source

cold side:
tube bending, cladding moves apart from inner heat source

(c) (f) burst cladding tube

FIG. 17 - Strain anisotropy and bending of Zircaloy-4 cladding tubes in the α-phase

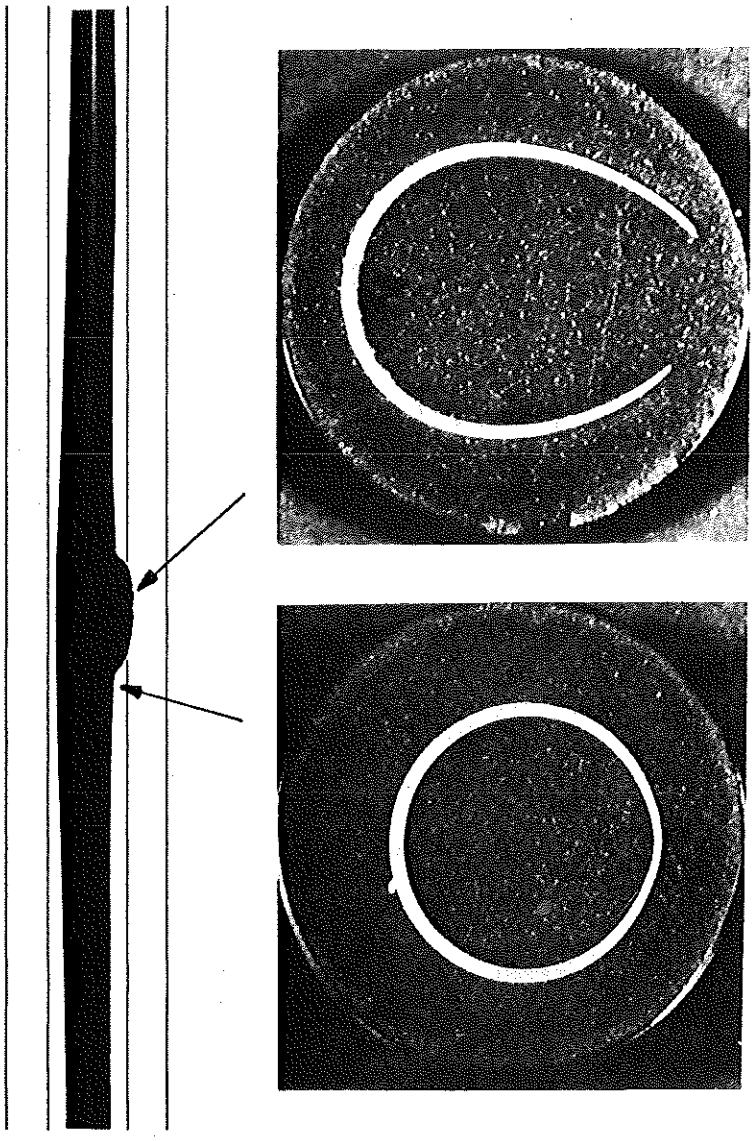

FIG. 18 - Bending of Zircaloy-4 cladding tube deformed under azimuthal temperature difference and cooling

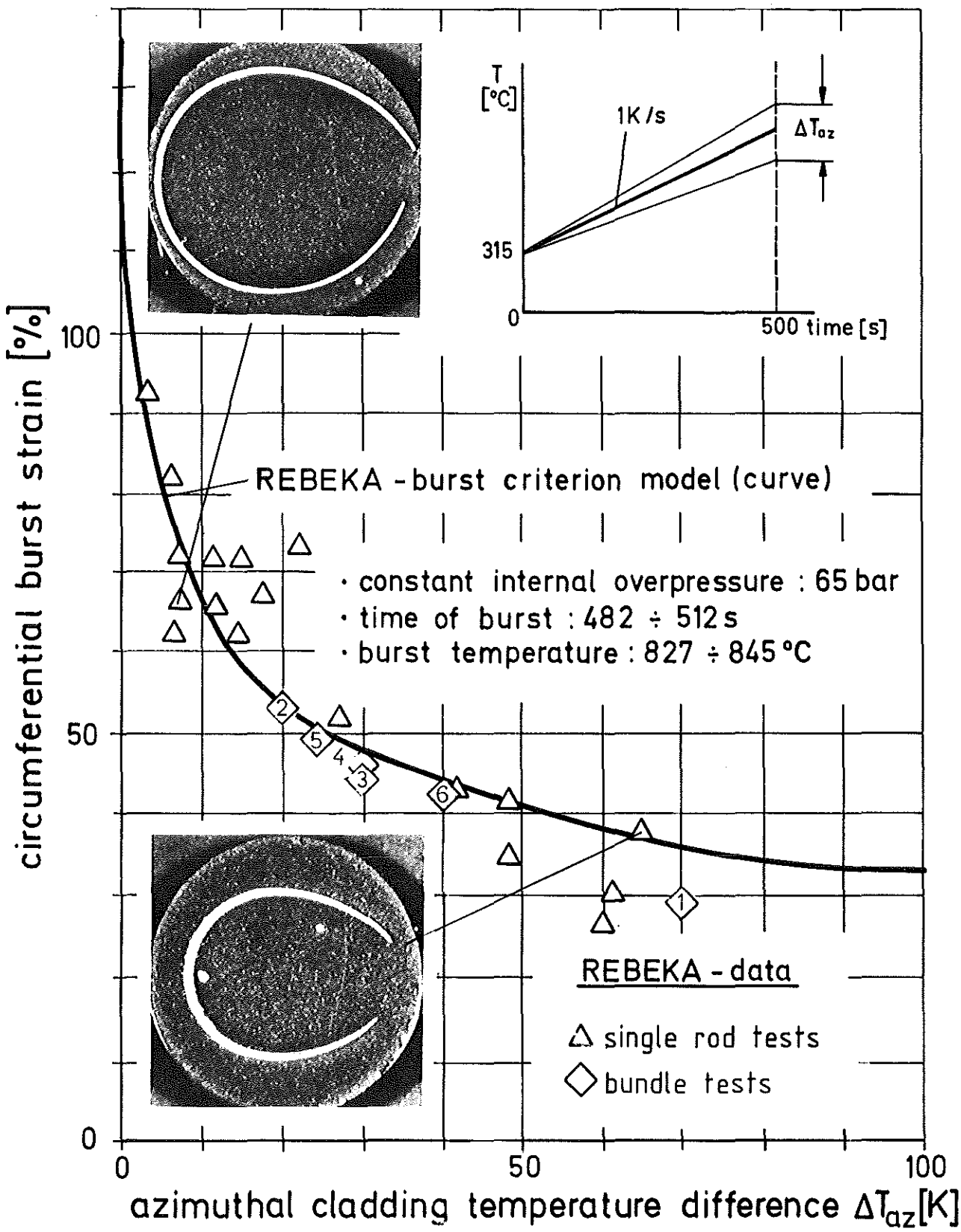

FIG. 19 - Burst strain of Zircaloy-4 cladding tubes versus azimuthal temperature difference (REBEKA tests)

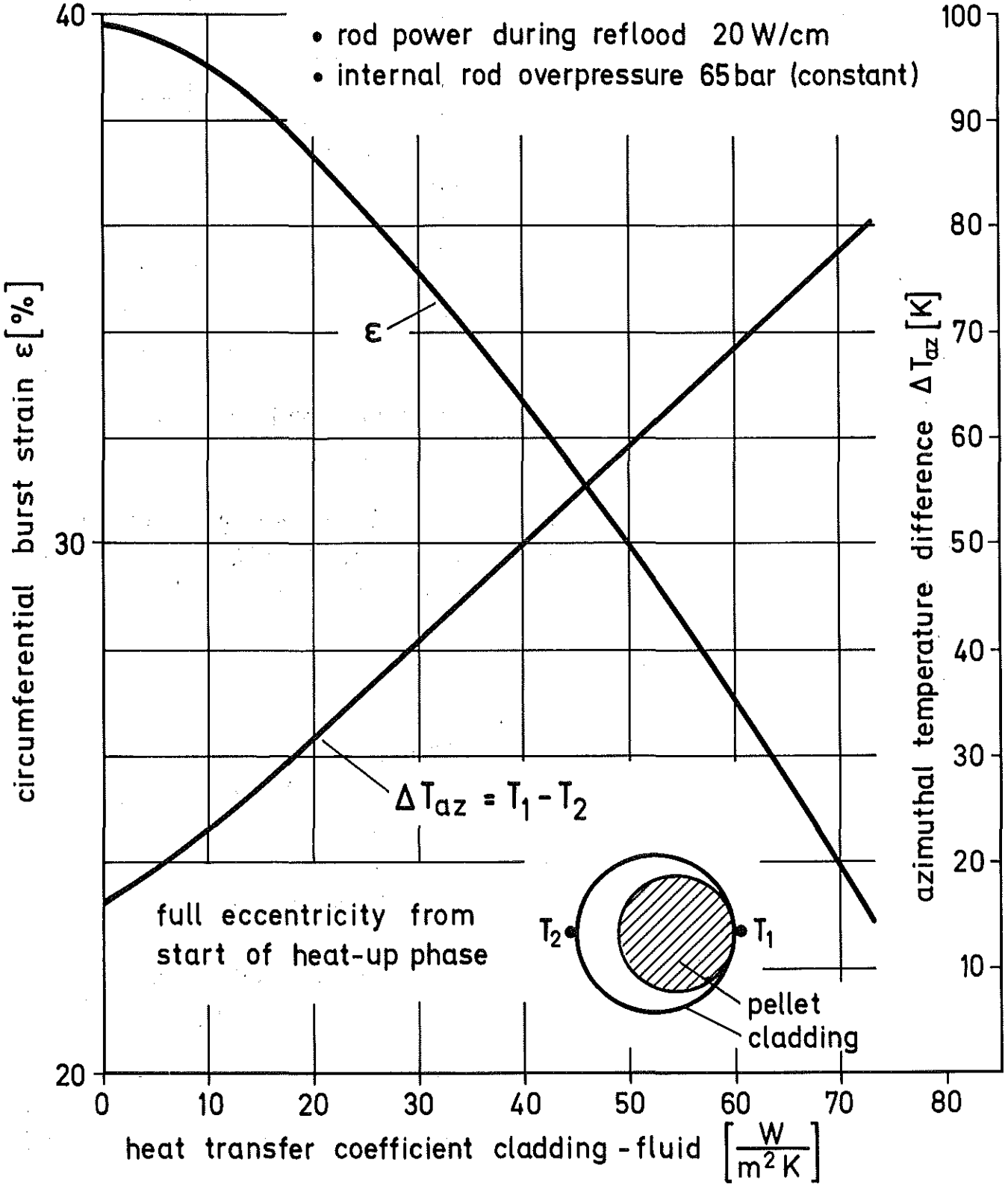

FIG. 20 - Influence of heat transfer on Zircaloy-4 cladding tube deformation

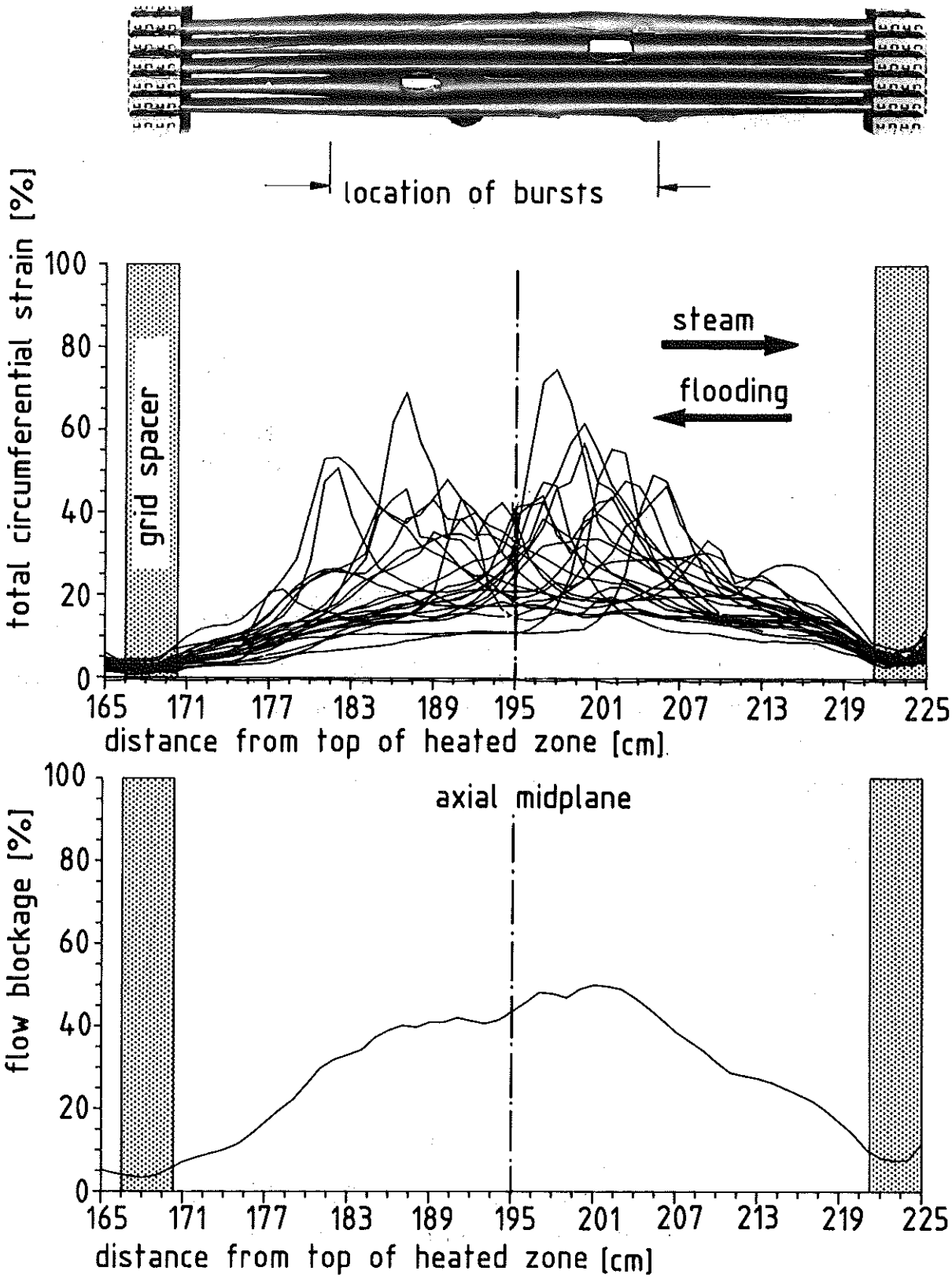

FIG. 21 - Zircaloy-4 cladding deformation and flow blockage under reversed flow (REBEKA 5)

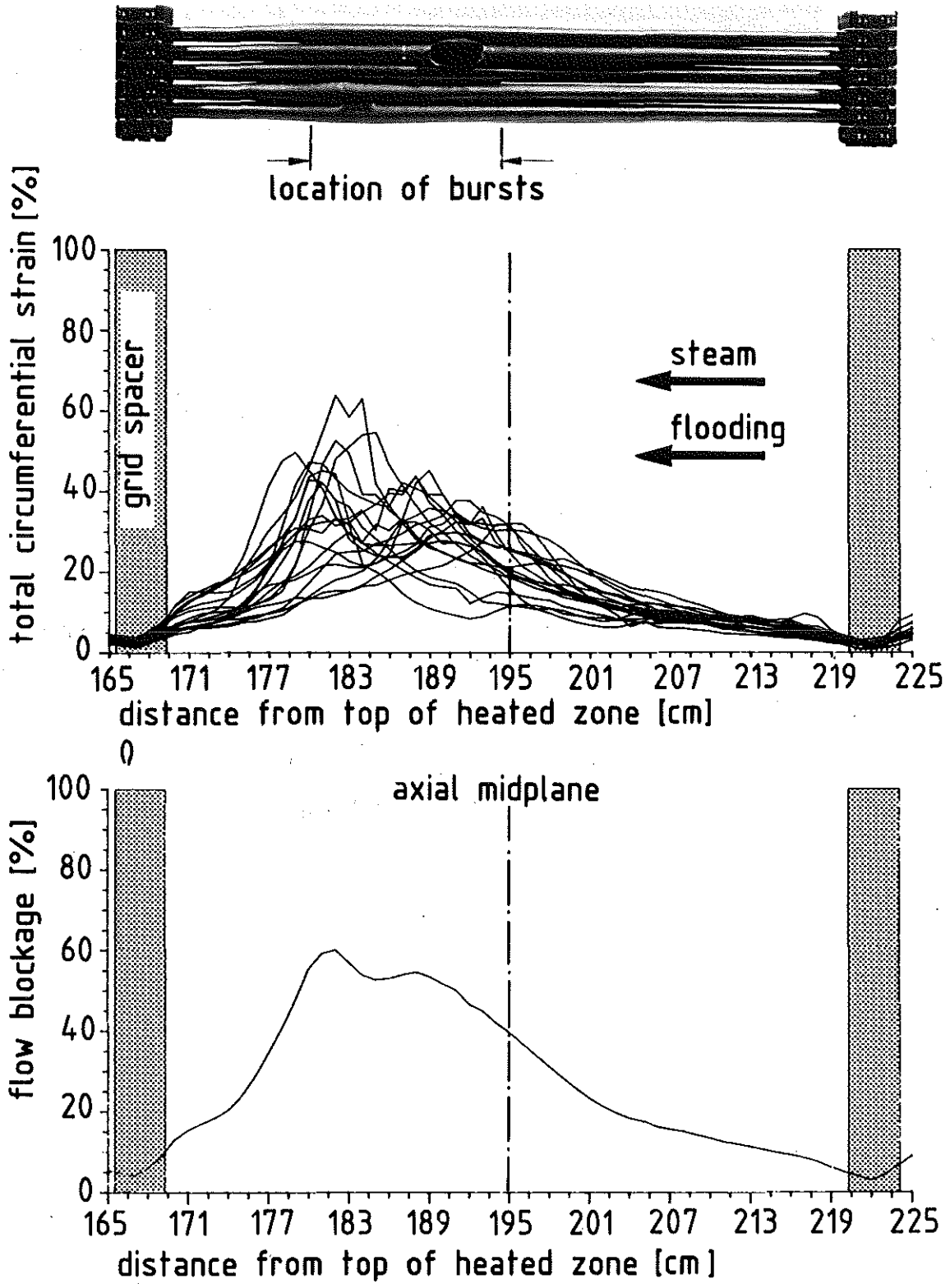

FIG. 22 - Zircaloy-4 cladding deformation and flow blockage under unidirectional flow (REBEKA 6)

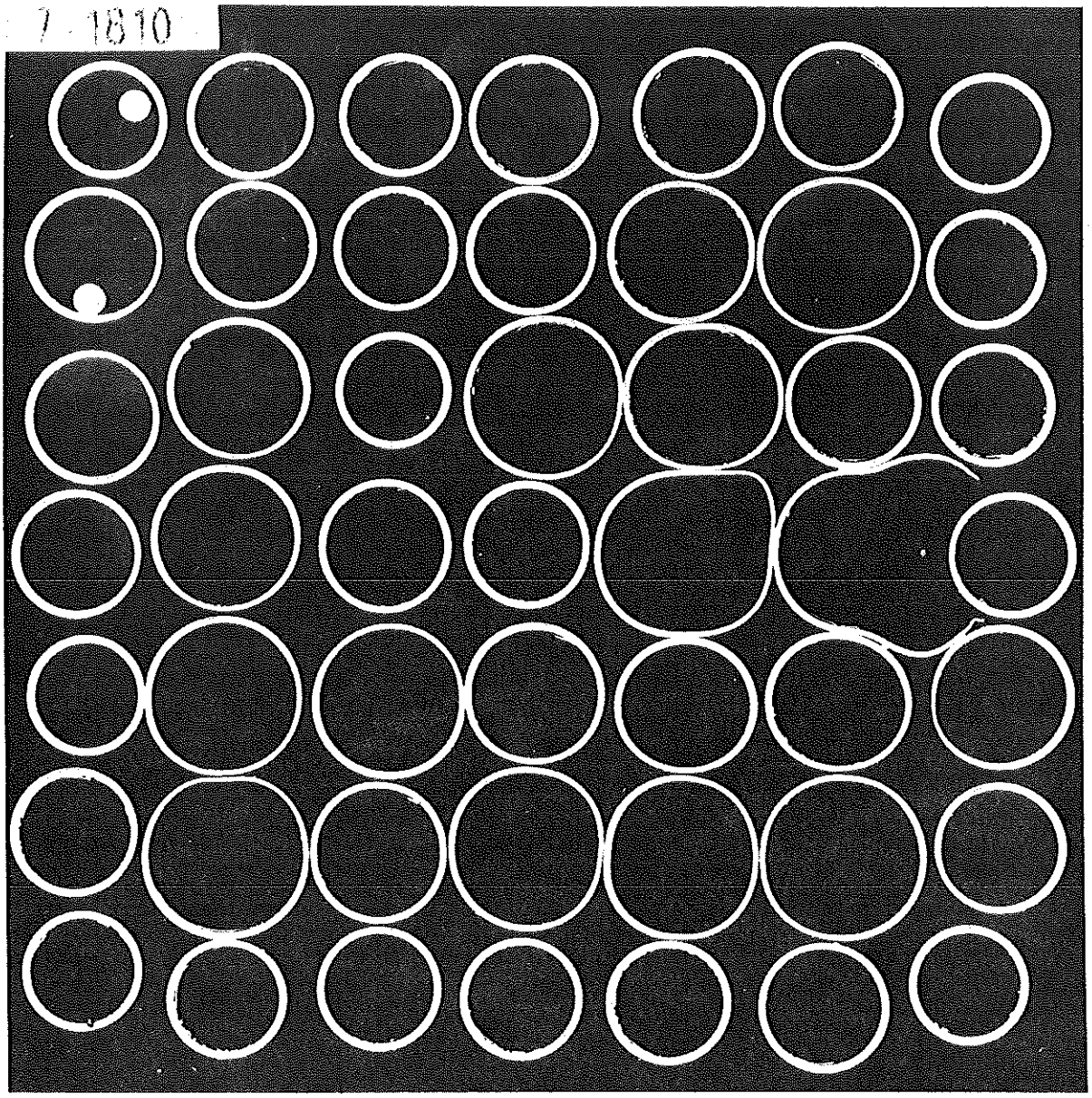

FIG. 23 - Bundle cross-section at maximum flow blockage (REBEKA 7)

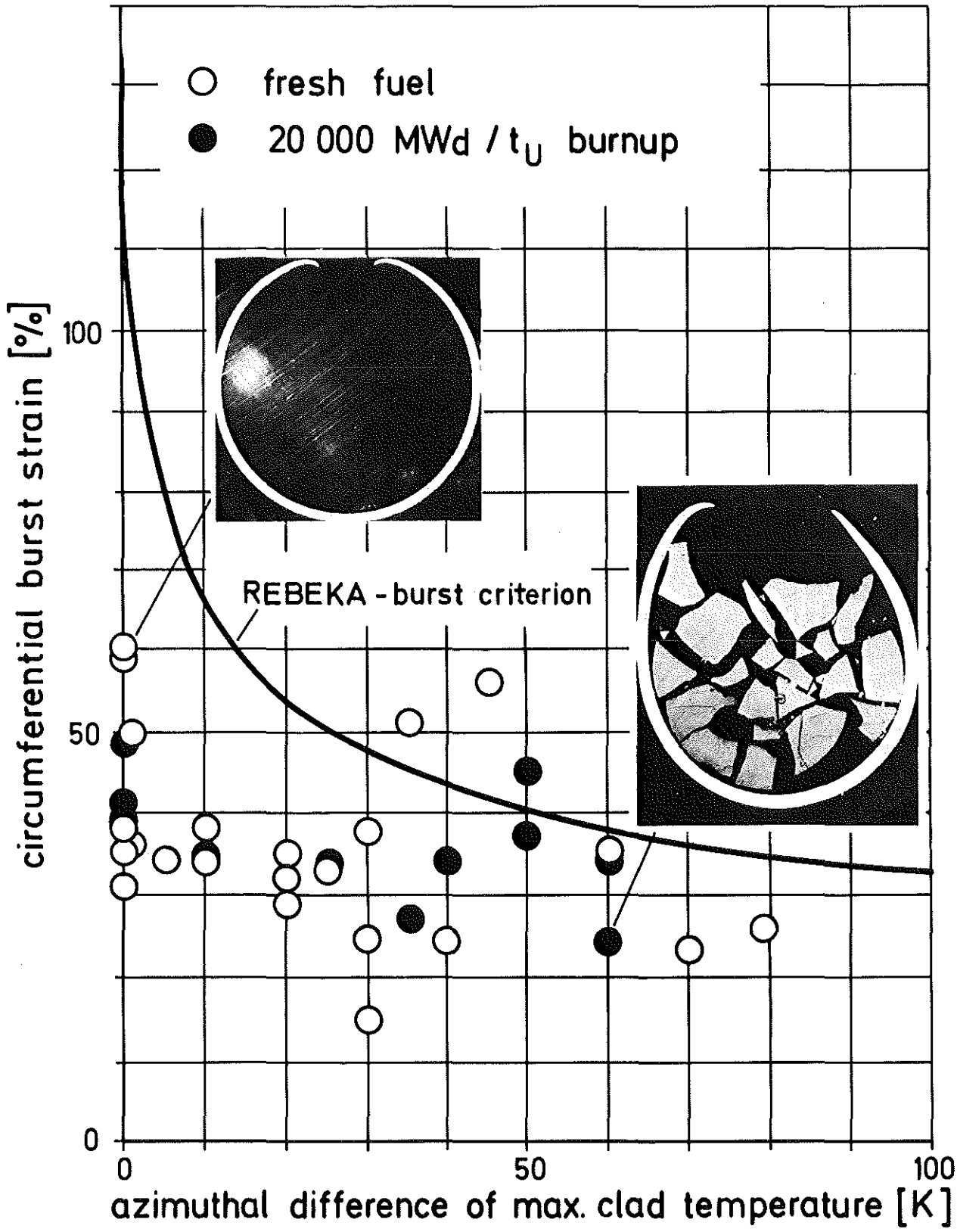

FIG. 24 - Burst strain of Zircaloy-4 cladding tubes versus azimuthal temperature difference (FR-2 in-pile versus REBEKA out-of-pile tests)

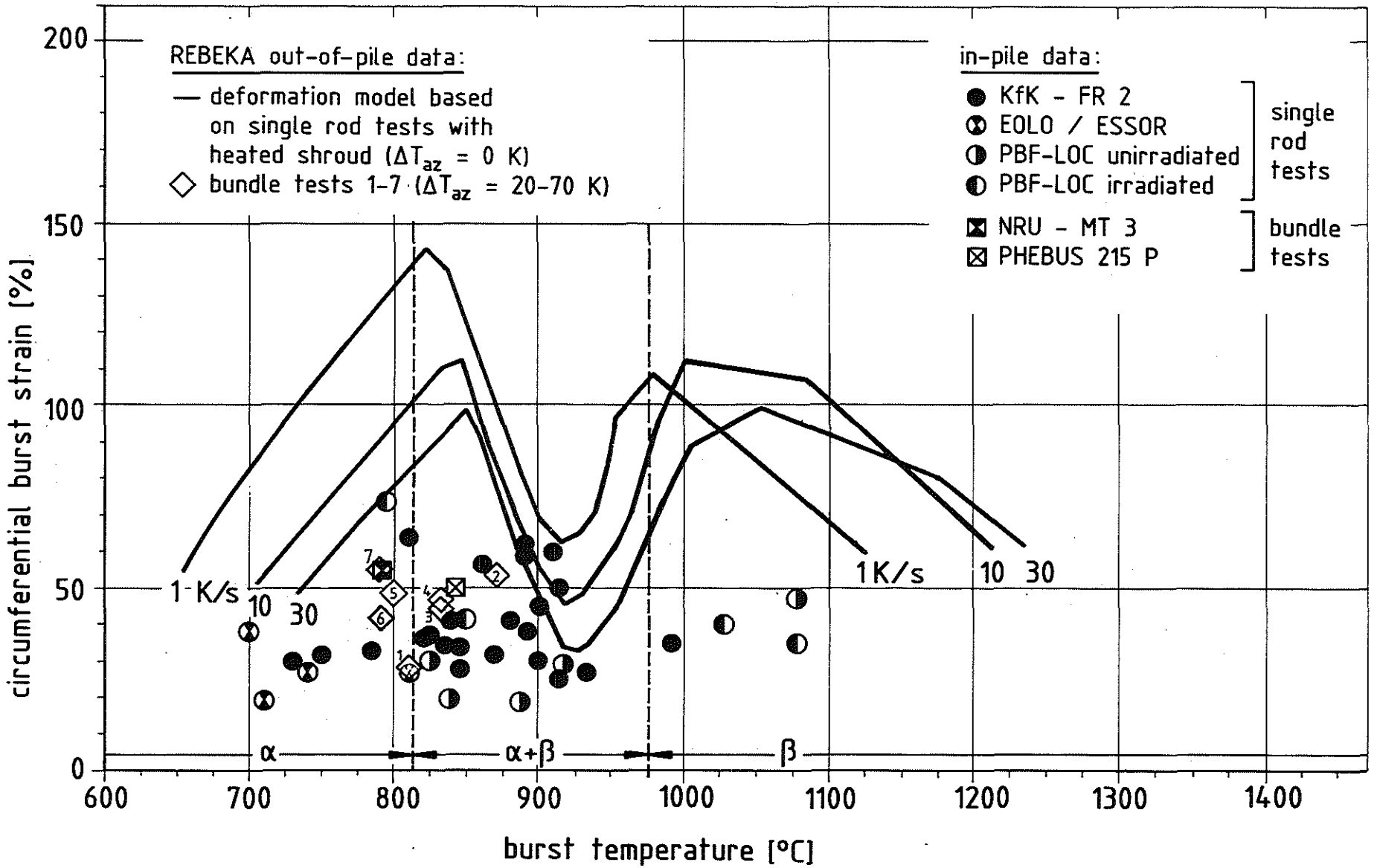

FIG. 25 - Burst strain versus burst temperature of Zircaloy-4 cladding tubes (in-pile vs. out-of-pile data)

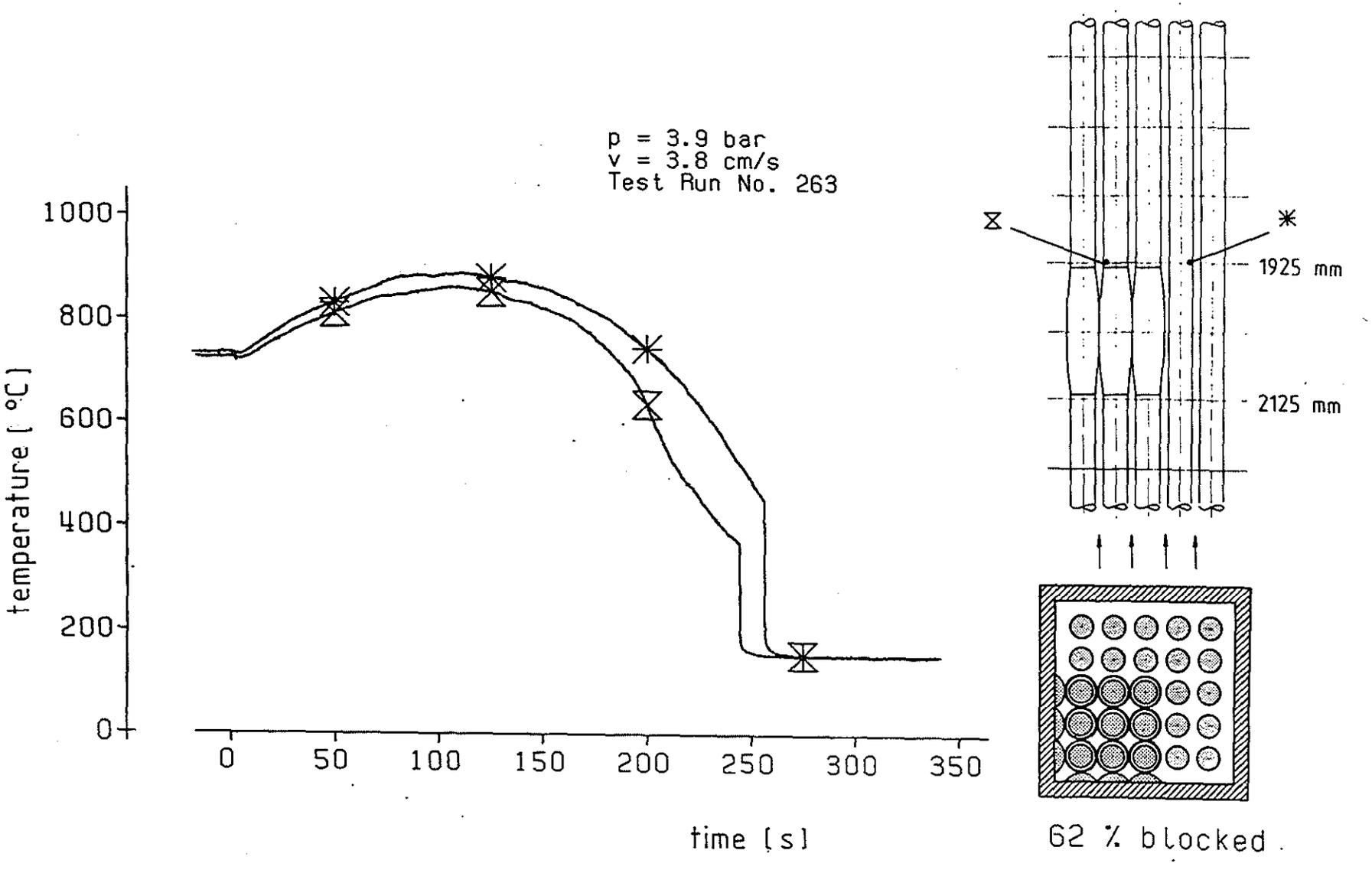

FIG. 26 - Cladding temperatures in a 62 % partly blocked bundle (FEBA tests)

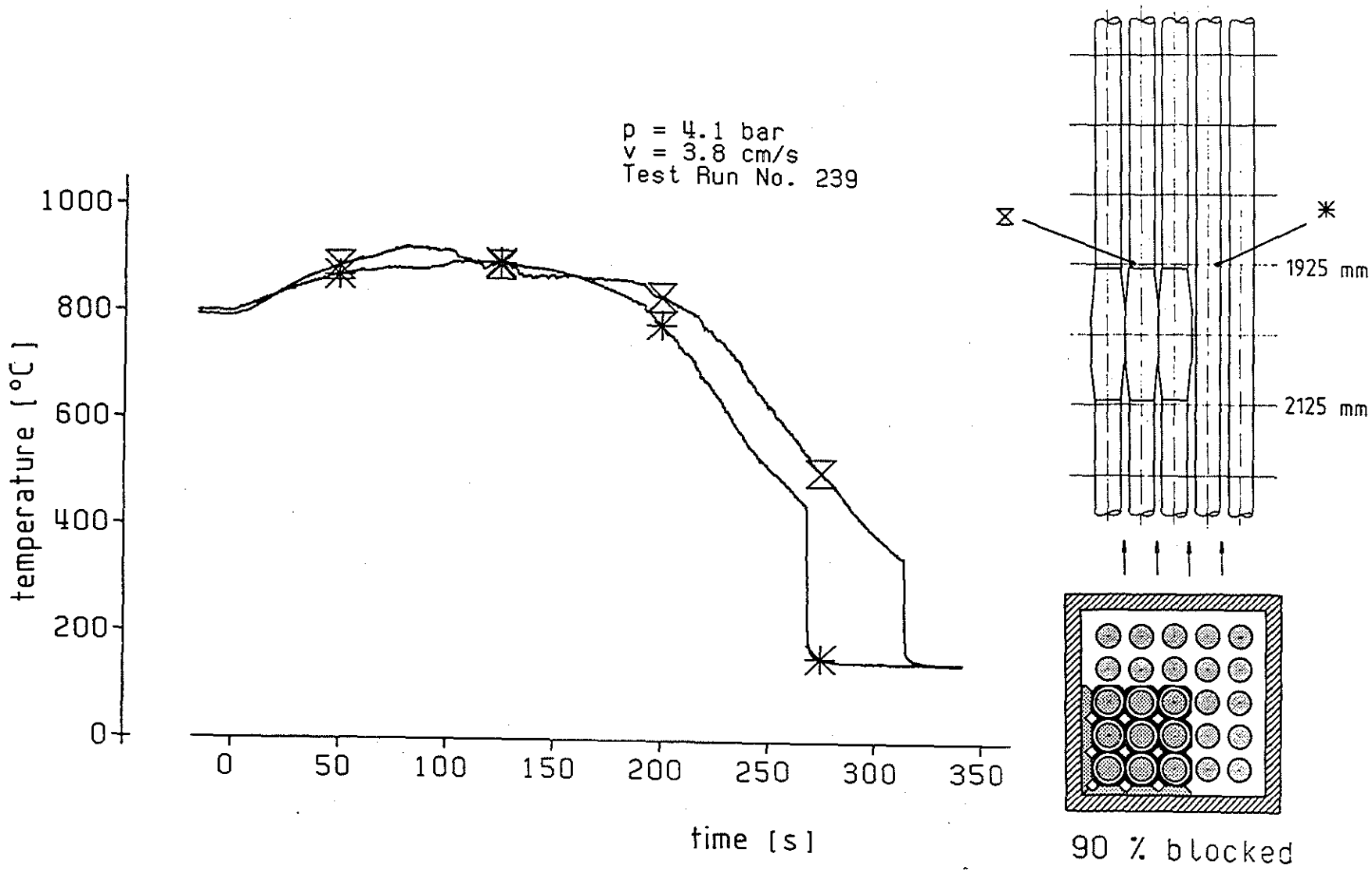

FIG. 27 - Cladding temperatures in a 90 % partly blocked bundle (FEBA tests)

TABLE I - LOCA simulation multi-rod burst tests

Tests			test geometry		thermal-hydraulic test conditions during cladding deformation				test results (averaged)				reference
			number of rods	heated length	heating rate	coolant flow	flow direction	heat transfer coefficient	burst temperature	burst strain	burst zone within grids	max. flow blockage	
				mm	K/s			$W/m^2 \cdot K$	°C	%	cm	%	
transient heatup tests (refill)	out - of - pile	JAERI -B 13	7×7 (all pressurized	850	<1	65 g/s m^2 steam	uni-directional	~2	782	~60	10	90	[65]
		MRBT -B 5	8×8 (all pressurized)	915	10	288 g/s m^2 steam	uni-directional	~5	768	60	40	90 (inner 4×4)	[66]
		KWU - 4	3×4 (2 pressurized)	650	9	forced air	uni-directional	60	838	52			[67]
	in - pile	PHEBUS - 215P	5×5 (all pressurized)	800	8	steam	uni-directional	50...90	840	50 (inner 3×3)	4	65	[68]
refill and reflood tests	in - pile	NRU -MT 3	6×6 w/o corner rods (12 pressurized)	3660	8.....1	steam / 5.6...1.0 cm/s reflood	uni-directional	60.....70	793	55	10	70	[69]
	out - of - pile	REBEKA -6	7×7 (all pressurized)	3900	7.....-4	~2m/s steam / ~3cm/s reflood	uni-directional	30...100	790	42 (inner 5×5)	14	60	[70]
		REBEKA - 5	7×7 (all pressurized)	3900	7.....0	~2m/s steam / ~3cm/s reflood	reversed from refill to reflood	30...100	800	49 (inner 5×5)	24	52	[71]

TABLE II - REBEKA multi-rod burst tests

test number	bundle size	thermal-hydraulics during cladding deformation				burst data (averaged)					max. flow blockage	remarks	reference
		heating rate	coolant flow	flow direction	heat transfer coefficient	temperature		pressure	circumferential strain	intergrid distribution of bursts			
		K/s			W/m^2K	3) °C	4)	bar	%	mm	%		
1	5x5	7[1]...<1[2]	•steam •reflood	reversed	30...100	685	810	60	28		25	• inner 3x3 pressurized • only 2 rods burst • high reflood rate at start of reflood	[72]
2		7[1]	steam	uni-directional	30	870	870	55	54	95	60	inner 3x3 pressurized	[73]
3		7[1]...<1[2]	•steam •reflood	reversed	30...100	808	830	51	44	203	52	inner 3x3 pressurized	[74]
4		7[1]...<1[2]		reversed	30...100	795	830	53	46	242	55	•inner 3x3 pressurized •control rod guide tube in centre	[75]
M		0	quasi-stagnant steam		<10	754	754	70	63	28	84	•1 W/cm •all pressurized •2 rods leaked	[76]
5	7x7	7[1]...0[2]	•steam •reflood	reversed	30...100	775	800	68	49	242	52	all pressurized	[71]
6		7[1]...-4[2]		uni-directional	30...100	765	790	62	42	140	60	•2 rods unpressurized •instrument tube in centre	[70]
7		7[1]...-9[2]		uni-directional	30...100	755	790	57	55	200	66	all pressurized	

common test conditions:

heated length: 3900 mm; decay heat at midpoint: 20 W/cm; axial peaking factor: 1.19; axial power profile: 7 axial steps (5x5 tests), cosine-shaped (7x7 tests), system pressure: 4 bar; coolant flow: ~2 m/s steam, ~3 cm/s forced flooding from bottom; Zircaloy-4 claddings: 10.75 x 0.72 mm, stress relieved

1) during heat up 2) during reflood in the time period of high plastic deformation before burst

3) measured nearest to burst at time of burst 4) best-estimate burst temperature

TABLE III – LOCA simulation reflood tests in blocked bundles

Tests	test and blockage geometry						thermal-hydraulic test conditions			results			reference
	number of rods	rod diameter	heated length	blockage ratio (coplanar)	number of fully blocked subchannels	blockage length incl. conical ends	forced feed cold flooding velocity	system pressure	rod power % ANS - standard	max. difference of peak clad temp. downstream of blockage: blockage/bypass	max. difference of peak clad temp. downstream of blockage: blocked/unblocked	max. difference of peak clad temp. blockage: sleeve/bypass	
		mm	m	%		mm	cm/s	bar	%	K	K	K	
FLECHT / SEASET	21	9.5	3.05	up to 90	up to 24	60 180	1...25	1.4...2.8	50...120	none or negative	none or negative	negative	[77]
	163	9.5			up to 48	60 180			120	none or negative	none or negative	negative	
SCTF	2000	9.5	3.66	62	~ 400	60	3... 10	~ 2.4	120	negative	no tests	negative	[78]
THETIS	49	12.2	3.58	90 80	9 9	450	1.3...5.8	1.3...4.1	30...50		no tests	positive, late about 100 K	[79]
FEBA	25	10.75	3.9	90	9	180	3.8...5.8	2...6	120	max. 50 K mostly none or negative	none	negative	[80]
				62	9	180	2... 10			none	negative	negative	